

LA-9369-MS

C.3

Los Alamos National Laboratory is operated by the University of California for the United States Department of Energy under contract W-7405-ENG-36.

CIC-14 REPORT COLLECTION
REPRODUCTION
COPY

*Transport in Connection with
the Hiroshima-Nagasaki
Dose Reevaluation Effort*



Los Alamos Los Alamos National Laboratory
Los Alamos, New Mexico 87545

This work was supported by the Defense Nuclear Agency.

DISCLAIMER

This report was prepared as an account of work sponsored by an agency of the United States Government. Neither the United States Government nor any agency thereof, nor any of their employees, makes any warranty, express or implied, or assumes any legal liability or responsibility for the accuracy, completeness, or usefulness of any information, apparatus, product, or process disclosed, or represents that its use would not infringe privately owned rights. References herein to any specific commercial product, process, or service by trade name, trademark, manufacturer, or otherwise, does not necessarily constitute or imply its endorsement, recommendation, or favoring by the United States Government or any agency thereof. The views and opinions of authors expressed herein do not necessarily state or reflect those of the United States Government or any agency thereof.

LA-9369-MS

UC-11 and UC-34c
Issued: July 1982

Air Transport in Connection with the Hiroshima-Nagasaki Dose Reevaluation Effort

G. P. Estes
R. C. Little
R. E. Seamon
P. D. Soran

Edited by
R. E. Seamon



Los Alamos Los Alamos National Laboratory
Los Alamos, New Mexico 87545

TABLE OF CONTENTS

| | PAGE |
|---|------|
| ABSTRACT | 1 |
| I. INTRODUCTION | 1 |
| II. CALCULATIONAL TOOLS | 3 |
| III. CALCULATIONS | 3 |
| A. APRD Reactor Experiments | 3 |
| B. Pulsed Sphere Calculations | 5 |
| C. ORNL Broomstick Experiments | 7 |
| IV. ATTEMPTS AT CROSS-SECTION MODIFICATIONS | 9 |
| A. Effect on ORNL Broomstick Results | 9 |
| B. Comparisons of ENDF/B-V Cross Sections with Other Sets | 10 |
| C. Effect on APRD Reactor Experiment Calculations | 11 |
| V. MODEL MODIFICATIONS | 14 |
| A. Geometry Model | 14 |
| B. Neutron Leakage Spectrum | 15 |
| VI. CONCLUSIONS | 15 |
| REFERENCES | 16 |
| FIGURES | 20 |
| TABLES | 61 |

AIR TRANSPORT IN CONNECTION WITH THE HIROSHIMA-NAGASAKI
DOSE REEVALUATION EFFORT

by

G. P. Estes, R. C. Little, R. E. Seamon, and P. D. Soran

Edited by

R. E. Seamon

ABSTRACT

During calendar year 1981 one man-year of effort on the part of the Monte Carlo Group at Los Alamos was committed to the renormalization of cross sections for use in air-over-ground calculations. Calculations of the Army Pulsed Reactor Division (APRD) measurements, the Oak Ridge National Laboratory (ORNL) "broomstick" experiments, and the Lawrence Livermore National Laboratory (LLNL) pulsed sphere experiments carried out with the view to renormalizing the air transport cross sections are described in this report. On the basis of our calculations, it is impossible to conclude that there is anything grossly in error with the air transport cross sections.

I. INTRODUCTION

"In reviewing the recent controversy¹⁻¹⁰ which has arisen regarding radiological effectiveness of neutrons and gamma rays based on Hiroshima data, it was agreed that past calculations on which the controversy hinges were inadequate and that a much better analysis of the source term and transport should be performed." (Quoted from Ref. 11). The Monte Carlo Group at Los Alamos has been involved in this effort through consultation on device transport cross sections and through air-over-ground cross-section normalization including comparisons with the Livermore pulsed sphere results^{12,13} and the measurements

made at the Aberdeen Proving Ground^{14,15} by various organizations using the APRD reactor as a source. This commitment on the part of the Monte Carlo Group to the effort of reevaluating the dosimetric factors based on the Hiroshima and Nagasaki bomb blasts was summarized in detail in Ref. 11.

In order to accomplish the tasks outlined in Ref. 11, the Monte Carlo Group has carried out calculations of various air transport benchmark experiments. Where disagreements between calculation and experiment were observed, cross-section modifications were attempted in an effort to match the calculation with experiment and to understand the physics of neutron transport in air.

The various benchmarks for which calculations have been performed are as follows.

Army Pulsed Reactor Division (APRD) Measurements^{14,15}
ORNL Broomstick Experiments^{16,17}
LLNL Pulsed Sphere Experiments^{12,13}

The results of these calculations will be discussed in detail in the following sections of this report.

A brief description of the chronology of the calculations is in order. First the APRD experiments were calculated. When the results did not agree particularly well with experiment, and when the previously observed discrepancies between calculated and experimental results for certain pulsed spheres were considered, it was decided to calculate simpler, benchmark-type experiments. The results from the ORNL broomsticks suggested that some modifications of the total cross sections of nitrogen and oxygen might be in order. Modifications, admittedly somewhat arbitrary, were made to the nitrogen and oxygen cross sections to obtain better agreement between calculation and experiment for the broomsticks. These modified cross-section sets were then used in the 1100-m APRD calculations to determine if agreement between calculation and experiment was improved.

Calculations of the LLNL pulsed spheres for air, oxygen, nitrogen, and water were done mainly because Mendelsohn and Loewe^{1,3} had used a calculation of a liquid air pulsed sphere as supporting evidence for their dosimetric work. However, it is not clear that these 14-MeV neutron experiments are particularly relevant to the transport of fission neutrons. This will be discussed in more detail later.

II. CALCULATIONAL TOOLS

Except as otherwise noted, the calculations were carried out using the continuous-energy Monte Carlo code MCNP.¹⁸ The cross sections in the format for MCNP were processed in the Nuclear Data Group by R. E. MacFarlane and R. M. Boicourt using the ACER module of NJOY.¹⁹ The cross sections for the MCNP calculations were derived basically from ENDF/B-V.²⁰ Modifications in the cross-section sets as described in this report were carried out in the Monte Carlo Group.

III. CALCULATIONS

We proceed now to describe the calculations of the various benchmark experiments.

A. APRD Reactor Experiments

In the APRD experiments performed at the Aberdeen Proving Grounds,^{14,15} the neutron and photon flux spectra from a fast critical assembly were measured in an air-over-ground environment. Measurements were made at distances ranging from 15 m to 1100 m, the latter distance being comparable to distances of interest in the Hiroshima and Nagasaki dose reevaluation effort. For this reason these measurements are well suited to serve as an air transport benchmark for the current studies.

An additional advantage of these experiments is that three different experimental groups have performed essentially identical measurements for some detector locations, thereby giving us an indication of the reproducibility of the results. Common measurements exist for detectors positioned at 100, 170, and 300 m. These independent measurements were carried out by the APRD,¹⁴ the Canadian Defence Research Establishment Ottawa (DREO),¹⁵ and a West German defense group (WWD).¹⁴ The DREO measured spectra at 15, 400, and 1100 m also.

Discrete ordinates (DOT-3) calculations have been performed by DREO and ORNL¹⁵ for these experiments. These calculations were made using the DLC-31 group structure;¹⁵ for convenience, all experimental results were presented in this group structure.

A schematic of the experimental arrangement is shown in Fig. 1. The reactor is mounted on a tower and can be raised to a height of 14 m. The detectors were mounted 2 m above the ground at the distances previously mentioned.

The experiments were not ideal from the viewpoint of terrain and weather conditions. At the 300- and 400-m positions, the detectors were positioned in a 20-m wide swath cut through a forested area. At 1100-m the detector was located at the top of a 25-m high hill. The atmospheric and ground conditions varied considerably during the various measurements. For example, during part of the WWD measurements, the ground was covered by snow (water equivalent of 35 l/m²) and it was raining (91% relative humidity). The specific weather data are given in Refs. 14 and 15.

All neutron spectrum measurements were made with NE213 detectors using pulse height discrimination and various unfolding techniques. It is the understanding of workers in the Monte Carlo Group, based on conversations with various experts, that such measurements are accurate only to about 15-20% on a spectral basis. The results of the three independent measurements at 100, 170, and 300 m support this contention. If the three individual measurements for a particular distance and energy bin are ratioed to the average of the three measurements, the results generally fall within a $\pm 20\%$ band over the entire energy spectrum. This is illustrated in Fig. 2 where these ratios are plotted versus energy for each of the three measurements and distances. The ratio for each energy bin is plotted at the midpoint of the bin, and the individual points are connected for clarity. It should be noted that this method of data presentation does not give an accurate visual representation of the total integral agreement since the energy bin widths vary considerably.

The neutron spectra obtained from the MCNP calculations at 15, 100, 170, 300, 400, and 1100 m are shown in Figs. 3 and 4. These same calculated spectra are compared to the experimental results in Figs. 5-9, one figure for each detector location. It should be noted that the calculated results are compared to the average of the three measurements in Figs. 5-7 and to the single available measurement in Figs. 8 and 9.

In order to interpret better the results of Figs. 5-9, these data are presented again in Figs. 10 and 11 (the heavy dashed lines) in a manner similar to that of Fig. 2; i.e., the results of the Monte Carlo calculations are ratioed to the measurements on a bin-by-bin basis. Along with the continuous-energy Monte Carlo calculations, the discrete ordinates calculations are compared with experiment in Figs. 10 and 11. In Fig. 10 the calculated results have been divided by the appropriate averages of the three independent measurements while in Fig. 11 the calculated numbers are divided by the only available experimental

results, those of the DREO. In Fig. 10 we see that the Monte Carlo calculations lie essentially within the experimental uncertainties over the entire energy range for the 100-m distance. At 170 m and 300 m (Fig. 10) and again at 400 m (Fig. 11) we see that the calculations are skewed too high at low energies and too low at high energies. That trend is not so evident at 1100 m, but instead we note that the significant over-calculation (or undermeasurement!!) at 5 MeV has become very pronounced.

Neutron KERMA measurements and calculations over the energy range 0.55-10 Mev are summarized in Table I as ratios of calculated and measured KERMA's to the DREO measured KERMA's. The Monte Carlo (MCNP) calculations (Col. 3) are higher than the discrete ordinates (DOT) calculations (Col. 2) as a function of detector location except at 1100 m. However, regardless of which type of calculation one carries out, the calculational ratios (Cols. 2 and 3) lie within the range of the experimental measurement ratios (Cols. 4 and 5) at the first three detector locations where independent measurements were made.

We discuss next simpler benchmark calculations and several modifications to nitrogen and oxygen cross sections. The effects of these modified cross sections on the APRD reactor neutron spectrum measurements are detailed later on in this report.

B. Pulsed Sphere Calculations

As part of an ongoing program in the Monte Carlo Group to assess the relative validity of various sets of nuclear cross sections and to help identify the relative strengths and weaknesses of various data sets, integral calculations²¹⁻²⁷ have been made of the Livermore Pulsed Sphere measurements.^{12,13} In the pulsed sphere experiments, the neutron time-of-flight spectra emitted from spherical targets bombarded with a central 14-MeV neutron source are measured. A schematic of the experimental geometry is shown in Fig. 12.

It is the time-of-flight spectra that we calculate. Although the conversion from time-of-flight to energy is approximate, the graphical results are presented as energy spectra for convenience of discussion. The calculated spectra are compared to the experimental results by ratioing the difference between calculated and experimental numbers to the experimental number; viz., $(C-E)/E$. We integrate this quantity over various energy ranges for use in comparisons. The intervals 2-5 MeV, 5-10 MeV, 10-13 MeV, 13-16 MeV, and 2-16 MeV were arbitrarily chosen for this purpose.

Calculations have been carried out using data from ENDF/B-IV, ENDF/B-V,²⁰ and the Livermore Evaluated Nuclear Data Library (ENDL).²⁸ In Table II a summary is given of all pulsed sphere results obtained using ENDF/B-V data. The total (C-E)/E ratio in percent is given for rough comparisons. We realize that such comparisons over the total energy range can be sometimes misleading because of compensating effects in various energy ranges.

Of particular interest for the air transport calculations are the results for hydrogen, nitrogen, and oxygen obtained using ENDF/B-V cross sections:

| | |
|------|-------------------------|
| H-1 | MAT=1301 from Tape 511 |
| N-14 | MAT=1275 from Tape 505 |
| O-16 | MAT=1276 from Tape 505. |

The pulsed sphere results for these three materials are summarized in greater detail in Table III, where the (C-E)/E ratios are given for four sub-energy intervals as well as for the total energy interval. Table III also serves as an index to Figs. 13-18. On each figure the calculated curves and the experimental data points are plotted versus neutron time-of-arrival at the detector and also versus neutron energy deduced from the time-of-arrival. The energy ranges for the integral comparisons are delineated on the lower plots in each of the figures.

A thoughtful inspection of the information contained in Table II along with the curves and tables of Refs. 21-27 will convince the reader that the agreement of the pulsed sphere data for N-14, O-16, and water is not as good as that for other materials. One rough comparison that can be made from the numbers available in this memo is offered. The average of the total $\left| \frac{(C-E)}{E} \right|$ for all experiments excepting N-14, O-16, and water is about 3.5 while the average of the total $\left| \frac{(C-E)}{E} \right|$ for N-14, O-16, and water is about 5. Of course, one can say that none of the pulsed sphere experimental results are fit perfectly, but the N-14, O-16, and water experiments are not fit as well as the others. This opinion is confirmed by calculations of the Livermore liquid air pulsed sphere experiment,²⁹ which were also carried out.³⁰ In Ref. 30 we have results using both ENDL-73 and ENDF/B-IV (essentially the same as ENDF/B-V) data. The calculations with ENDF/B-IV do not agree well with experiment or with the ENDL-73 calculations as shown in Table IV. With ENDF/B-IV we overcalculate this experiment in the 3-7 MeV range--the same phenomena we observe with the N-14,

0-16, and water pulsed spheres as documented in Table III. It is this consistent disagreement which led to the suggestion that there was something wrong with the cross sections for air and also to the suggestion that these cross sections should be reexamined. In fact, the Los Alamos Nuclear Data Group, which is responsible for the nitrogen and oxygen evaluations, would be willing to reexamine the ENDF/B-V evaluations in the 14-MeV range on the basis of the availability of new data.

However, for the APRD calculations, the 14-MeV data are not so important, but instead it is the energy range of the fission spectrum that is of concern. It seemed that if the nitrogen and oxygen cross sections were to be readjusted, this should be accomplished using some relatively clean experiments--experiments for which both the measured and calculated results could be obtained with relative ease and some certainty. The oxygen¹⁶ and nitrogen¹⁷ broomstick experiments were chosen. These experiments are among the dozen or so which are used in data testing carried out by the Cross-Section Evaluation Working Group (CSEWG), which program is summarized in detail in a report edited by R. W. Roussin.³¹

C. ORNL Broomstick Experiments

In the "broomstick" experiments the nitrogen or oxygen sample was contained in a glass dewar 4 in. in diameter and several feet in length (3 ft for nitrogen and 5 ft for oxygen). The axis of the long, narrow cylinder (i.e., a broomstick) coincided with the axis of the neutron beam which was confined to a diameter of 3.5 in. by collimators placed between the neutron source (Tower Shielding Reactor II) and the sample. In order to reduce the effect of neutron in-scattering in the sample, the distance from the neutron source to the sample was 50 ft and the detector was 50 ft from the sample. The uncollided transmitted spectrum was measured with and without the target material in the dewars. The resolution function of the system and the unfolding procedure are given in the benchmark write-ups^{16,17} so that a smeared calculated spectrum can be compared directly to the reported experimental spectrum.

Calculations of the shielding benchmarks SDT2¹⁶ and SDT3¹⁷ have been carried out using ENDF/B-V cross sections and several sets of modified nitrogen and oxygen cross sections.

To calculate the Oak Ridge broomstick experiments with MCNP including a fine enough energy structure (>200 energy bins) takes a nontrivial amount of

computer time. Therefore, a code which calculates the experiments analytically was written. The code is useful for quick checks of effects of cross-section modifications.

The code simply calculates the transmitted flux, $\phi(E)$, as

$$\phi(E) = S(E)e^{-n\sigma_t(E)}$$

at 10,000 energies equally spaced from 0.5 to 12.0 MeV. The source at energy E , $S(E)$, is interpolated from the source distribution given in Table I of the SDT reports.^{16,17} The total cross section, $\sigma_t(E)$, is interpolated from the appropriate ACE cross-section file. The sample thickness, n , is in atom/barn. The code assumes that once a neutron is scattered, it leaves the beam forever. This is a good assumption because of the geometry of the experiment.

To compare calculation with experiment, the transmitted flux must be broadened by the resolution function specified:

$$R(E' \rightarrow E) = \frac{93.944}{aE'} \exp\left\{-\left[\frac{(E' - E)235.482}{E'a}\right]^2 / 2\right\},$$

where a (in units of percent) is the full-width at half-maximum at energy E' . Values of $a(E')$ can be interpolated from Table II of the SDT reports.

The output from this code has been compared with results from 30-min MCNP runs to show that the results are consistent. Results also show favorable agreement with recent calculations by Rose at Brookhaven National Laboratory.³¹

Some results for the nitrogen and oxygen broomsticks are shown in Figs. 19-21 where the results of our calculations have been plotted onto curves copied from Refs. 16 and 17. The broad bands correspond to the experimental data. J. Briesmeister learned in 1981 from experimentalists at ORNL that the experimental information in numerical form has been destroyed, so that these graphs are the only representations of the experimental results available to us. The crosses indicate the results for calculations using ENDF/B-V cross sections while the dots represent the results for another set of cross sections deliberately modified to force a good fit to these broomstick measurements. We

should like to point out what changes in the total cross section were necessary to effect the good agreement with the broomstick curves.

IV. ATTEMPTS AT CROSS-SECTION MODIFICATIONS

A. Effect on ORNL Broomstick Results

In Fig. 19 the crosses correspond to results of calculations using ENDF/B-V cross sections for N-14 (MAT=1275 from ENDF/B-V Tape 505), and the dots represent the results obtained when σ_{tot} was changed from ENDF/B-V over eight energy intervals as shown in Fig. 22. These changes are summarized in Table V.

The modifications were arrived at after several trials were made in which the cross sections were changed--principally in the cross-section minima. All changes in the total cross section were reflected in similar changes in the elastic cross section to preserve cross-section balance in the Monte Carlo runs made subsequently with these files. The resulting elastic cross section is shown in Fig. 23.

In Fig. 20 the crosses correspond to the ENDF/B-V cross-section results while the dots represent results obtained when σ_{tot} was changed from ENDF/B-V--the changes having been arrived at in a different way. Rather than changing selectively around cross-section maxima and minima, the total cross section was changed uniformly by varying percentages over five broad energy intervals as summarized in Table VI and shown in Fig. 24.

We note that the percent changes given in Tables V and VI are significantly outside the $\pm 1\%$ uncertainties suggested in Ref. 32 by Young and Foster, who prepared the ENDF/B-V evaluation for nitrogen.

Similar work was carried out for O-16. In Fig. 21 the crosses correspond to results of calculations using ENDF/B-V cross sections for O-16 (MAT =1276 from ENDF/B-V Tape 506), and the dots represent the results obtained when σ_{tot} was changed from ENDF/B-V over three energy intervals as summarized in Table VII and shown in Fig. 25.

Once again we note that the changes in the total cross section required to effect the good agreement with experiment (as shown in Fig. 21) are significantly outside the $\pm 1\%$ uncertainties suggested in Ref. 33 by Foster and Young, who prepared the ENDF/B-V oxygen evaluation.

The very large changes in σ_{tot} with which we must deal lead one to raise the question as to whether the experimental data given by the broad bands in

Figs. 19-21 are really correct. On the basis of their work the evaluators, Young and Foster, cannot approve such radical cross-section modifications.

When the question of validity of the experiments was raised at the November 30, 1981 meeting of the Shielding Data Testing and Applications Subcommittee of the CSEWG and the results shown in Figs. 20 and 21 were presented, R. E. Maerker (the author of the writeups for the SDT2 and SDT3 benchmarks) stated that the ENDF/B-V predictions were very good and that there were no problems. The 50% discrepancy at 1.75 MeV and the factor of 2 at 3.75 MeV for N-14 were accepted without question as was the factor of 2 around 4.25 MeV for O-16. Maerker pointed out that in comparison with broomstick experiments for other materials, the agreement for N-14 and O-16 is excellent. The consensus seemed to be that it was foolish to be modifying the nitrogen and oxygen total cross sections because the agreement with the broomstick experiments is excellent using ENDF/B-V.

B. Comparisons of ENDF/B-V Cross Sections with Other Sets

There are other reasons to be suspicious of such large changes in the total cross sections. Consider N-14, for example. Here are five sets of cross sections for N-14 from among those available to the MCNP code:

| ZAID | Source | Temperature (°K) |
|---------|------------------|------------------|
| 7014.01 | ENDL-73 | 0.0 |
| 7014.02 | LAMDF (LRL-1970) | 0.0 |
| 7014.04 | ENDF/B-IV | 0.0 |
| 7014.30 | ENDL-76 | 0.0 |
| 7014.50 | ENDF/B-V | 300.0 |

The total cross sections from these sets are plotted together in Figs. 26 and 27. The data as found in ZAID=7014.01, 7014.02, and 7014.30 are all essentially the Livermore ENDL evaluation; it has remained relatively stable across the years. The N-14 evaluation from ENDF/B-V is the same as that for ENDF/B-IV except for updating of the covariance data format. Only on the expanded scale in Fig. 27 can one detect differences between the ENDL and the ENDF/B evaluations. One sees there evidence of the practice in ENDL of representing the data with as few points as possible. Broomstick results obtained using the five sets

of cross sections are tabulated in Table VIII where again it is confirmed that there are only two distinct sets of cross sections and that the results are essentially the same, especially if they would be plotted together in Figs. 19 or 20.

Similar comparisons were made for five of the 0-16 cross-section sets from among those available to the MCNP code:

| Z A I D | Source | Temperature (°K) |
|---------|-----------------|------------------|
| 8016.01 | ENDL-73 | 0.0 |
| 8016.02 | LAMDF(LRL-1971) | 0.0 |
| 8016.04 | ENDF/B-IV | 0.0 |
| 8016.30 | ENDL-76 | 0.0 |
| 8016.50 | ENDF/B-V | 300.0 |

Once again from plots of the cross sections and from broomstick results, one can confirm that there are clearly two distinct sets of cross sections — the ENDF/B and the ENDL evaluations. It is instructive to compare the cross sections in the energy range over which they were changed: 1 - 8 MeV. In Figs. 28 and 29 the total cross sections for 0-16 from ENDF/B-V, ENDL-76, and the new modification are compared. Clearly, the modified σ_{tot} values lie significantly outside any differences that exist between the widely accepted ENDL and ENDF/B evaluations.

C. Effect on APRD Reactor Experiment Calculations

Whatever the merits or demerits of the nitrogen and oxygen broomstick experiments may be, Tables V-VII and Figs. 22-29 serve to define five sets of cross sections used in various calculations to be subsequently discussed:

| | |
|---------------|-----------------|
| N-14 ENDF/B-V | Z A I D=7014.50 |
| N-14 N14F | Z A I D=7014.73 |
| N-14 N14FF | Z A I D=7014.86 |
| 0-16 ENDF/B-V | Z A I D=8016.50 |
| 0-16 016F | Z A I D=8016.73 |

Let us now address the question of how much of an effect the modifications in the nitrogen and oxygen total and elastic cross sections had on the calculations of the APRD reactor experiment.

In Figs. 30-33 there are plots of the neutron flux at 1100 m. It is helpful to compare Fig. 30 with the lower half of Fig. 11. The histogram values of the solid curve calculated by MCNP using the ENDF/B-V data divided by the histogram experimental values (dotted curve) in Fig. 30 are plotted at the midpoint of the histogram interval in Fig. 11 with the dotted curve. Note that between 4.965 and 6.376 MeV the experimental and calculated results are almost identical leading to the point near unity at 5.67 MeV. Between 7.408 and 8.187 MeV the calculated value is only 0.57 times the experimental number leading to the point plotted in Fig. 11 at 7.80 MeV.

In Fig. 31 we have the neutron flux at 1100 m calculated with the modified nitrogen and oxygen cross-section sets N14FF and O16F. We note immediately that the good agreement between calculation and experiment in the energy ranges $2.385 \leq E \leq 3.012$ MeV and $4.965 \leq E \leq 6.376$ MeV has been destroyed. The disagreement is increased in the energy range $4.066 \leq E \leq 4.724$ MeV. Agreement is improved somewhat in the energy range $7.408 \leq E \leq 8.187$ MeV. An indication of the overall change caused by the modified cross-section sets is given by the calculated KERMA's from 0.55-10.0 MeV. With the ENDF/B-V evaluations the KERMA was overcalculated by 17% (Table I); with the modified evaluations the KERMA was overcalculated by 27%.

Figures 32 and 33 are aids to better understanding these results incorporating the same information available in Figs. 30 and 31. In Fig. 32 the calculation with ENDF/B-V and modified cross sections are compared, and in Fig. 33 the two sets of calculations are compared with experiment. The neutron flux spectra at 1100 m show the largest effects of changing the nitrogen and oxygen cross sections. The differences between the N14F and N14FF cross-section sets were barely discernible, especially at distances 300 m and below.

In Figs. 10 and 11 the neutron spectrum measurements compared to experiment are plotted for each of the five detectors. One is struck by the growth of the peak near 5 MeV as the detector distance is increased. It would seem that too many neutrons were getting through at this energy. There is in the N-14 total cross section a window at 5 MeV; refer to Fig. 24 for a good plot over that energy range. To confirm that this window was responsible for the neutrons getting through as observed in the calculations, two sets of cross sections

were prepared as shown in Fig. 34. In the first set, N14FFF with ZAIID=7014.87, the cross sections between 4.6 and 5.2 MeV were modified to change the minimum from the ENDF/B-V value of 1.02 b to 1.31 b. In the second set, N14FFFF with ZAIID=7014.88, the cross sections between 4.2 and 5.2 MeV were changed to remove the peak at 4.6 MeV and to raise the minimum at 4.85 MeV from 1.02 b to 1.45 b as shown in Fig. 34. When the calculations at 1100 m were repeated using these modified cross sections, the peak in transmitted neutrons did not appear in the results--thus confirming the suspicion that it was this window in the N-14 σ_{tot} which was responsible for the effect. It is not clear why this effect was not observed in the experimental results, but it is present in both Monte Carlo (MCNP) and discrete ordinates (DOT) calculations.

In Figs. 10 and 11 at distances 170, 300, and 400 m, we seem to overpredict in the energy range 0.5-2.5 MeV while in the range 5.0-11.0 MeV it appears that we underpredict. Various sets of N-14 and O-16 cross sections were prepared starting from ENDF/B-V. The total cross section was multiplied by some factor over an energy range; the elastic cross section was changed appropriately. The cross-section files are described in Table IX. Even these large changes in cross sections do not bring calculation and experiment into agreement:

- 1) Drastic decreases of 20% in the total cross section of nitrogen (5-11 MeV) produced the following increases in calculated flux from 5-11 MeV: 3% at 100 m, 7% at 170 m, and 14% at 300 m. These changes should be compared with discrepancies between base-case calculation and average experiment of 14%, 25%, and 15% at the respective distances over the same energy range.
- 2) In the energy range from 0.5502 to 1.827 MeV, we overcalculated the average experiment by 22% at 100 m, 21% at 170 m, and 37% at 300 m. By increasing the cross sections of both oxygen and nitrogen by 5% in this energy range, we decreased the calculated results by only 3%, 2%, and 2%. Twenty percent increases in the cross sections decreased the calculated results by 9%, 13%, and 16%.

It is interesting to note that when broomstick calculations were made using the two oxygen files, the results could have been tolerated when plotted on Fig. 21. However, the nitrogen results when plotted on Figs. 19 or 20 must be regarded as unacceptable. At high energies the results are a factor of 2 higher or lower when N14RL1 or N14RL2 are used, and at low energies file N14RL4 produces results which are only 40% as large as the results from ENDF/B-V.

V. MODEL MODIFICATIONS

Besides the importance of assorted changes in the air transport cross sections, studies have been made of the importance of changes in the specifications of the APRD reactor model as well.

Specifically, the importance of changes in the density of the ground, the moisture content of the ground, the relative humidity of the air, and the source spectrum have been investigated.

A. Geometry Model

The MCNP geometry model used for calculations up to the 400-m detector position is shown in Fig. 35. The various geometrical regions defined were used for the variance reduction techniques of geometry splitting and Russian roulette. For the 1100-m calculations this geometry was modified to provide for more splitting in the vicinity of the detector. The air compositions used in the calculation reflected the relative humidity at the time of the measurements.

The ground was represented in these models but is not visible on the scale of Fig. 35. A 10-cm depth of ground was assumed and four surfaces were used for splitting in the depth dimension. The ground composition for all detector locations was assumed to be the average of the "wet" and "dry" compositions given in Ref. 14.

The effects on the flux spectrum of ground water, ground density, and relative humidity of the air are shown in Figs. 36-39.

In Fig. 36 the flux at 300 m is shown as calculated using the two extremes of "wet" and "dry" ground composition as given in Ref. 14.

In Fig. 37 the effect of changes in ground density on the flux at 300 m is demonstrated. The change by nearly a factor of 2 in ground density effects changes in the flux that lie within the statistical uncertainties of the calculation.

In Figs. 38 and 39 the importance of the relative humidity on the spectrum at 100 m and 300 m is demonstrated. The extremes of the changes in humidity produce changes that can be significantly larger than the statistical uncertainties of the calculations but still within the uncertainties of the measurements.

Insofar as the calculated KERMA's (0.55 MeV-10 MeV) are concerned, similar changes in the ground water, ground density, and relative humidity of air each had an effect of no more than 6% at 300 m.

B. Neutron Leakage Spectrum

The neutron leakage spectrum from the APRD reactor used as a source in the MCNP calculations was taken from Appendix I of Ref. 15 (same as Annex A of Ref. 14). This spectrum has itself been calculated³⁴ with MCNP using physical characteristics from Refs. 15 and 35. To determine the leakage spectrum the flux is tallied over all surfaces of the reactor cylinder. The results are given in Table X where the leakage fraction from Ref. 15 is compared with the calculated leakage fraction for each of 31 energy groups ranging from ≈ 100 eV to ≈ 20 MeV. Ratios of the calculated leakage fraction to the tabulated values are given also. Typical Monte Carlo statistical errors (one standard deviation) are listed as well. The MCNP calculation shows about 20% more leakage above 3 MeV and 20% fewer neutrons below 0.5 MeV.

The neutron spectrum calculations for all five detector distances were repeated using the neutron leakage spectrum from Table X as the source in MCNP. The results are compared with the previously discussed MCNP and DOT calculated results in Figs. 40 and 41, where it is seen that the transmitted spectrum is consistently higher corresponding to the substantially higher reactor leakage spectrum in the energy range 2-10 MeV.

The agreement between the calculated and experimental KERMA values (such as those summarized in Table I) is worse when the calculated neutron leakage spectrum from Table X is used as the source in the MCNP KERMA calculation. For example, at detector locations 100-400 m, the calculated KERMA (0.55 MeV-10 MeV) increase by $\approx 15\%$ while at 1100 m the calculated KERMA increases by $\approx 30\%$.

VI. CONCLUSIONS

The "broomstick" experiments are well calculated in the viewpoint of those whose opinion on these matters might well be trusted. Furthermore, modifications to the cross-section data that would be required to fit perfectly the "broomstick" data are outlandish and should not be entertained as possibilities.

The nitrogen, oxygen, and liquid air pulsed spheres are not calculated as well as one would like. There is a lack of agreement between the calculations of the Lawrence Livermore National Laboratory (TARTNP) and the Los Alamos National Laboratory (MCNP) when these pulsed sphere experiments are calculated using what are supposed to be the same cross-section sets. These differences have been with us for years and may have something to do with differences in the

processing and implementation of evaluated data sets. It is essential for workers at both laboratories to be supported in the tasks of understanding and eliminating such differences. We do not believe that the air transport cross sections themselves are causing the differences.

Our calculations of the APRD reactor agree reasonably well with experimental results in an integral sense. However, the spectral agreement is not good--we overcalculate experiment at low energies (below ≈ 2 MeV) and undercalculate experiment at high energies (above ≈ 5 MeV). This type of spectral disagreement has been noted in previous calculations.^{14,15} We are not happy with the spectral results, but we feel that no reasonable changes in either the physical model of the problem or the nuclear data would resolve the discrepancies. We recommend looking elsewhere for the source of the discrepancies and are interested in further interactions with the experimentalists as they plan and analyze future measurements.

We feel that there are problems with oxygen and nitrogen transport data near 14 MeV. For fission spectrum neutrons, however, we feel that our calculations have not definitively confirmed or denied the validity of the air transport cross sections. We do have confidence in the basic nuclear data used in oxygen and nitrogen evaluations, and we do have confidence in the evaluations themselves. We feel that the uncertainties in these data as applied to Hiroshima air transport calculations are relatively small and will be overshadowed by uncertainties in other facets of the overall dose calculations.

REFERENCES

1. W. E. Loewe and E. Mendelsohn, "Revised Estimates of Dose at Hiroshima and Nagasaki and Possible Consequences for Radiation-Induced Leukemia," Lawrence Livermore National Laboratory report D-80-14 (September 11, 1980).
2. Eliot Marshall, "New A-Bomb Studies Alter Radiation Estimates," *Science* 212, 900 (May 22, 1981).
3. William E. Loewe and Edgar Mendelsohn, "Radiation Kermas at Hiroshima and Nagasaki," Lawrence Livermore National Laboratory report D-81-10 (May 31, 1981).
4. G. D. Kerr, "Review of Dosimetry for the Atomic Bomb Survivors," paper presented at the Fourth Symposium on Neutron Dosimetry, Gesellschaft fuer Strahlen-und Umweltforschung, Munich-Neuherberg, June 1-5, 1981.

5. Eliot Marshall, "New A-Bomb Data Shown to Radiation Experts," *Science* 212, 1364 (June 19, 1981).
6. William E. Loewe, "Revised Hiroshima and Nagasaki Dose Estimates," Lawrence Livermore National Laboratory E+TR (August, 1981).
7. Christopher J. Fitzgerald, "Varying Views on Low-Dose Radiation," *Nuclear News* 24, 64 (August, 1981).
8. Christopher J. Fitzgerald, "Revised A-Bomb Data Leads to Controversy," *Nuclear News* 24, 130 (August, 1981).
9. Bertram M. Schwarzschild, "Studies Revise Dose Estimates of A-Bomb Survivors," *Physics Today* 34, 17 (September, 1981).
10. Eliot Marshall, "Japanese A-Bomb Data Will Be Revised," *Science* 214, 31 (October 2, 1981).
11. Paul Whalen and Paul Robinson, "Hiroshima-Nagasaki Calculations," Los Alamos National Laboratory internal memorandum to Distribution (July 14, 1981).
12. C. Wong, J. D. Anderson, P. Brown, L. F. Hansen, J. L. Kammerdiener, C. Logan, and B. Pohl, "Livermore Pulsed Sphere Program: Program Summary through July 1971," Lawrence Livermore Laboratory report UCRL-51144, Rev. 1 (February 10, 1972).
13. W. Webster and C. Wong, "Measurements of the Neutron Emission Spectra from Spheres of N, O, W, U-235, U-238, and Pu-239, Pulsed by 14-MeV Neutrons," Lawrence Livermore Laboratory report UCID-17332 (December 15, 1976).
14. A. H. Kazi, C. R. Heimbach, R. D. Harrison, L. Schaenzler, and F. W. Buchholz, "Measurements of the Free Field Radiation Environment at the APRD Reactor," Materiel Testing Directorate of the Aberdeen Proving Ground report APG-MT-5279 (July 1979).
15. H. A. Robitaille and B. E. Hoffarth, "A Comparison of Measured and Calculated Air-Transported Radiation from a Fast, Unshielded Nuclear Reactor," Defence Research Establishment Ottawa (Canada) report No. 835 (December, 1980).
16. R. E. Maerker, "SDT2. Oxygen Broomstick Experiment - An Experimental Check of Neutron Total Cross Sections," Oak Ridge National Laboratory report ORNL-TM-3868 (ENDF-167) (September 1972).
17. R. E. Maerker, "SDT3. Nitrogen Broomstick Experiment - An Experimental Check of Neutron Total Cross Sections," Oak Ridge National Laboratory report ORNL-TM-3869 (ENDF-168) (September 1972).
18. Los Alamos Monte Carlo Group, "MCNP - A General Monte Carlo Code for Neutron and Photon Transport, Version 2B," Los Alamos National Laboratory manual LA-7396-M, Revised (April 1981).

19. R. E. MacFarlane, R. J. Barrett, D. W. Muir, and R. M. Boicourt, "The NJOY Nuclear Data Processing System: User's Manual," Los Alamos Scientific Laboratory manual LA-7584-M (December 1978).
20. D. Garber, C. Dunford, and S. Pearlstein, Editors, "ENDF-102 Data Formats and Procedures for the Evaluated Nuclear Data File, ENDF," Brookhaven National Laboratory report BNL-NCS-50496 (ENDF-102) (October, 1975).
21. G. P. Estes, "Pulsed Sphere Calculations with ENDF/B-V Cross Sections, (for transmittal to CSEWG)," Los Alamos Scientific Laboratory internal memorandum to R. E. MacFarlane (October 24, 1979).
22. G. P. Estes and J. S. Hendricks, "Integral Testing of Some ENDF/B-V Cross Sections," Trans. Am. Nucl. Soc. 33, 679 (1979).
23. G. P. Estes and R. E. Seamon, "Pulsed Sphere Calculations with ENDF/B-V Cross Sections (for transmittal to CSEWG)," Los Alamos Scientific Laboratory internal memorandum to P. G. Young and R. E. MacFarlane (May 9, 1980).
24. G. P. Estes and R. E. Seamon, "More Integral Testing of ENDF/B-V Data," Trans. Am. Nucl. Soc. 35, 460 (1980).
25. G. P. Estes, R. C. Little, R. E. Seamon, and P. G. Young, "Tools for Examining ENDF/B Data Prepared for Monte Carlo Calculations," Trans. Am. Nucl. Soc. 38, 568 (1981).
26. G. P. Estes, R. C. Little, R. E. Seamon, E. D. Arthur, and P. D. Soran, "Calculations Using New Tungsten Isotope Evaluations," Trans. Am. Nucl. Soc. 39, 794 (1981).
27. G. P. Estes, R. C. Little, and R. E. Seamon, "ENDF/B-V Data Testing for H, N, and O," Los Alamos National Laboratory memorandum to Robert W. Roussin, Chairman, CSEWG Shielding Data Testing and Applications Subcommittee (November 23, 1981).
28. R. J. Howerton, D. E. Cullen, R. C. Haight, M. H. MacGregor, S. T. Perkins, and E. F. Plechaty, "The LLL Evaluated Nuclear Data Library (ENDL): Evaluation Techniques, Reaction Index, and Description of Individual Evaluations," Lawrence Livermore Laboratory report UCRL-50400 Vol. 15 Part A (September 1975).
29. G. S. Sidhu, W. E. Farley, L. F. Hansen, T. Komoto, B. Pohl, and C. Wong, "Transport of Neutron and Secondary Gamma Radiations Through a Liquid Air Sphere Surrounding a 14-MeV Neutron Source," Nucl. Sci. Eng. 66, 428 (1978).
30. Guy Estes, "Preliminary Pulsed Sphere Calculations for Liquid Air," Los Alamos National Laboratory internal memorandum to Paul Whalen (January 14, 1981).

31. R. W. Roussin, Editor, "Shielding Data Testing and Applications Subcommittee of CSEWG - Contribution to the ENDF/B-V Data Testing Report," (in preparation).
32. P. G. Young and D. G. Foster, Jr., "An Evaluation of the Neutron and Gamma-Ray Production Cross Sections for Nitrogen," Los Alamos Scientific Laboratory report LA-4725 (ENDF-173) (September 1972).
33. D. G. Foster, Jr. and P. G. Young, "A Preliminary Evaluation of the Neutron and Photon-Production Cross Sections of Oxygen," Los Alamos Scientific Laboratory report LA-4780 (ENDF-174) (August 1972).
34. R. C. Little, "Calculation of APRD Reactor," Los Alamos National Laboratory internal memorandum to P. P. Whalen (January 21, 1982).
35. A. H. Kazi, "Experimental Radiation Transport to Large Distances from a Bare Reactor," Trans. Am. Nucl. Soc. 28, 634 (1978).

APRD Reactor Experiments

Provides test of neutron/photon transport and photon production in air over ground environment

Transport through humid air over wet ground.
Fission source neutrons and photons.
Pulse height measurement of spectra.

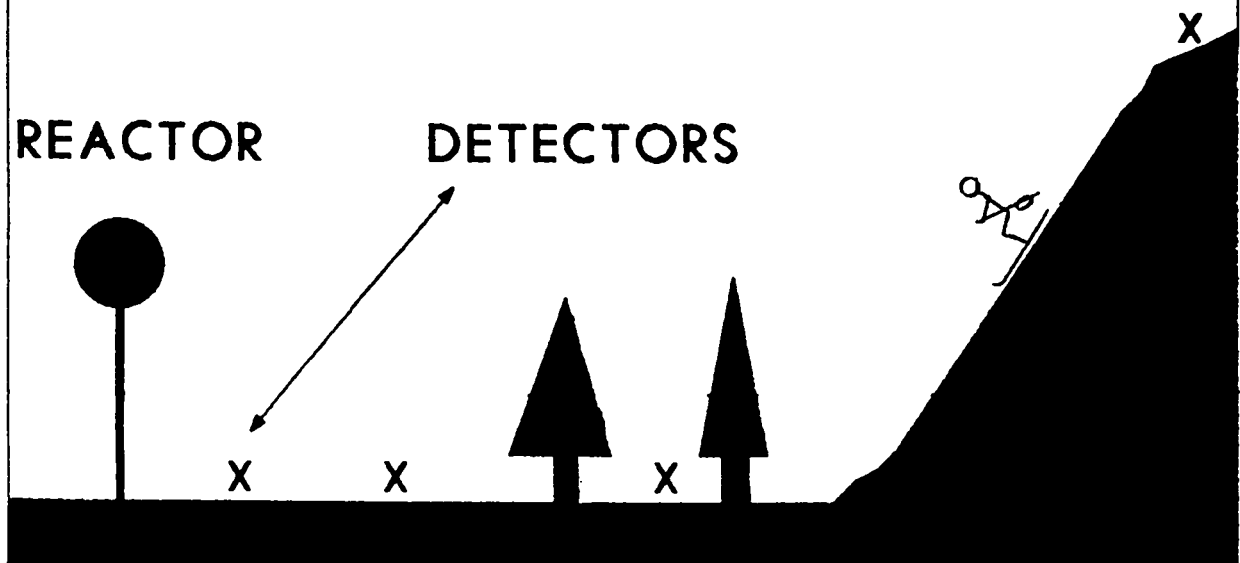


Fig. 1. Schematic of APRD reactor experiment.

APRD REACTOR NEUTRON SPECTRUM MEASUREMENTS

EXPERIMENT VS. EXPERIMENT AVERAGE

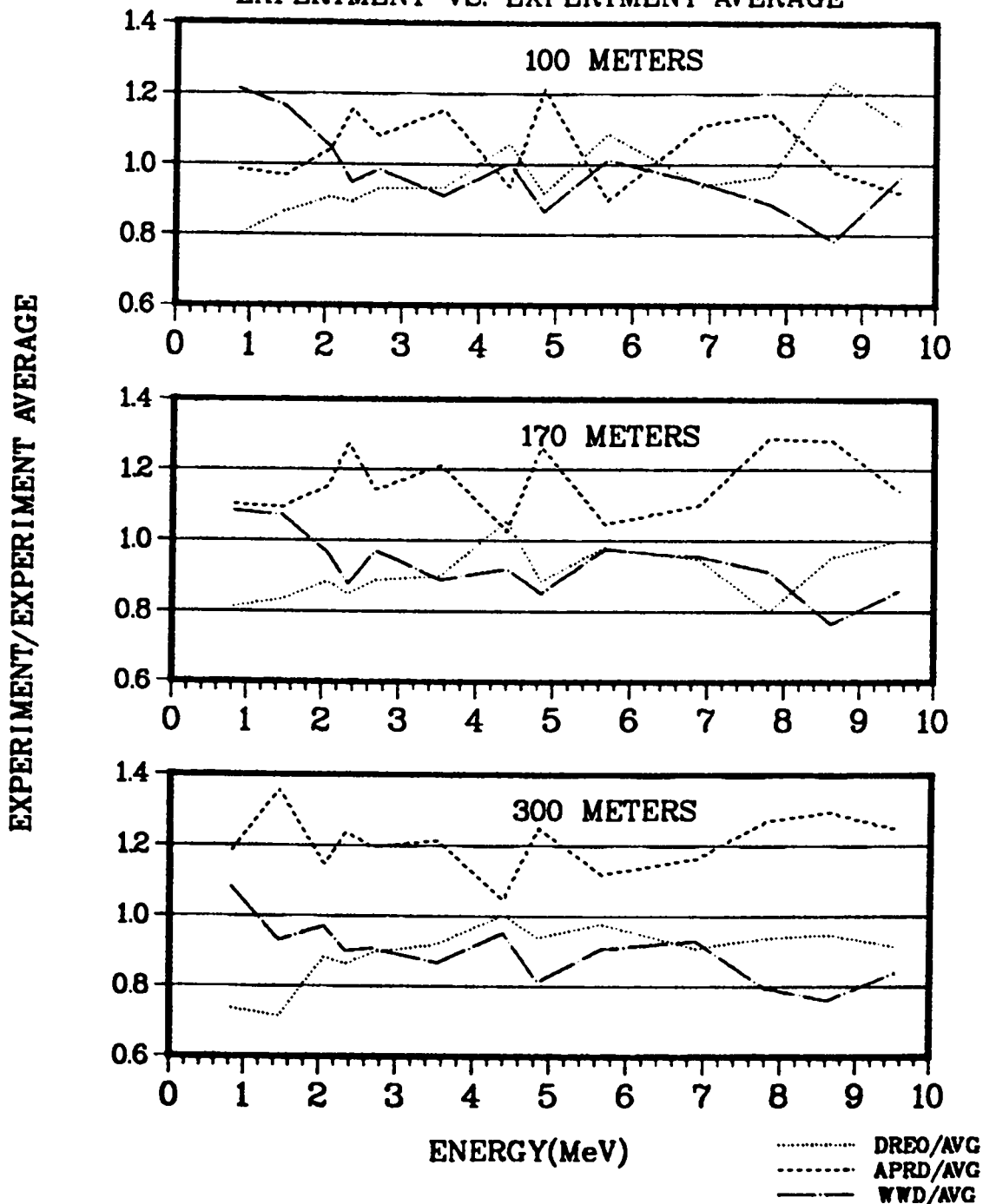


Fig. 2. Ratio of neutron spectrum measurements to average of experimental measurements.

NEUTRON FLUX AT 15 METERS

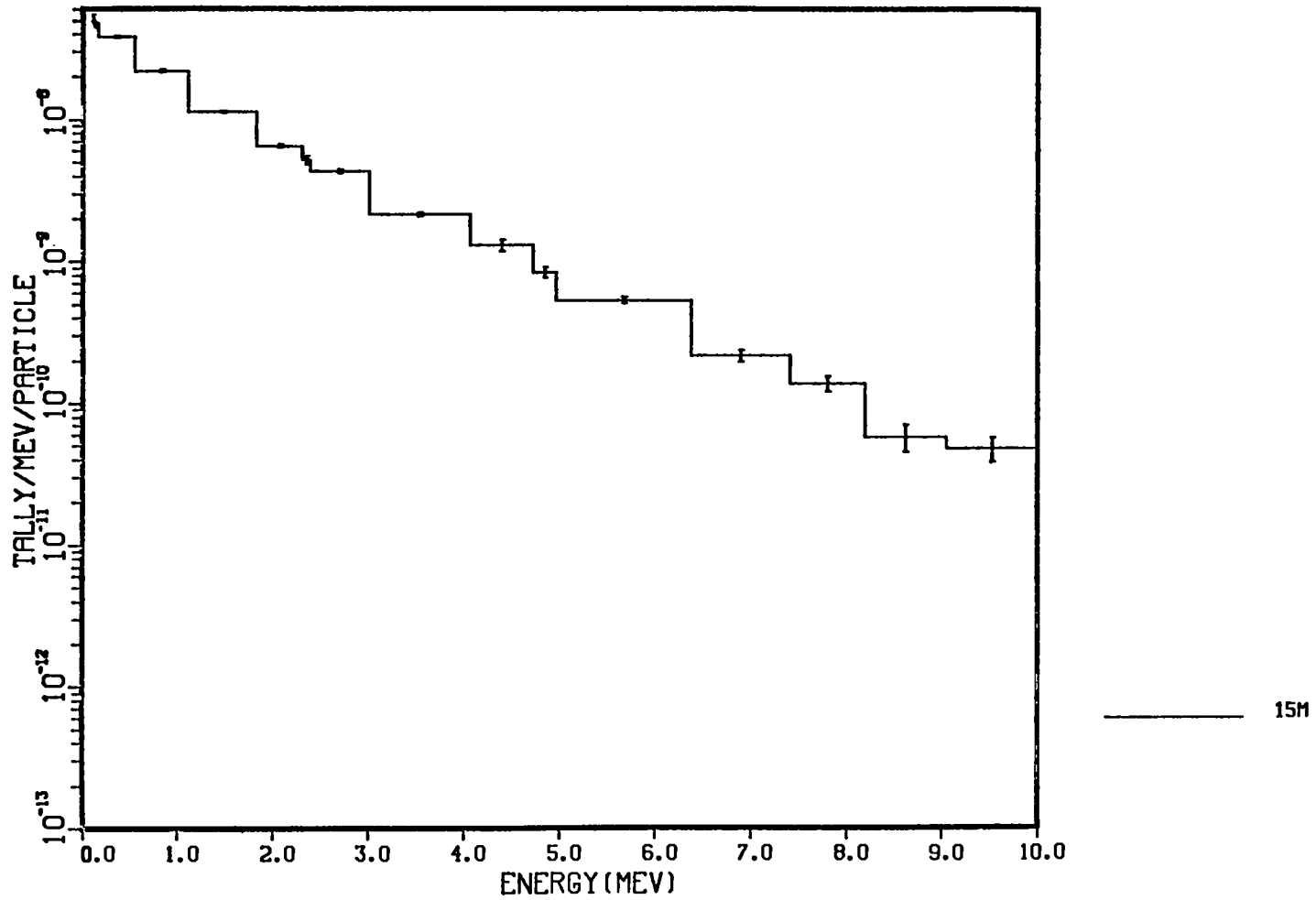


Fig. 3. Neutron flux at 15 m.

CALCULATED APRD NEUTRON SPECTRA

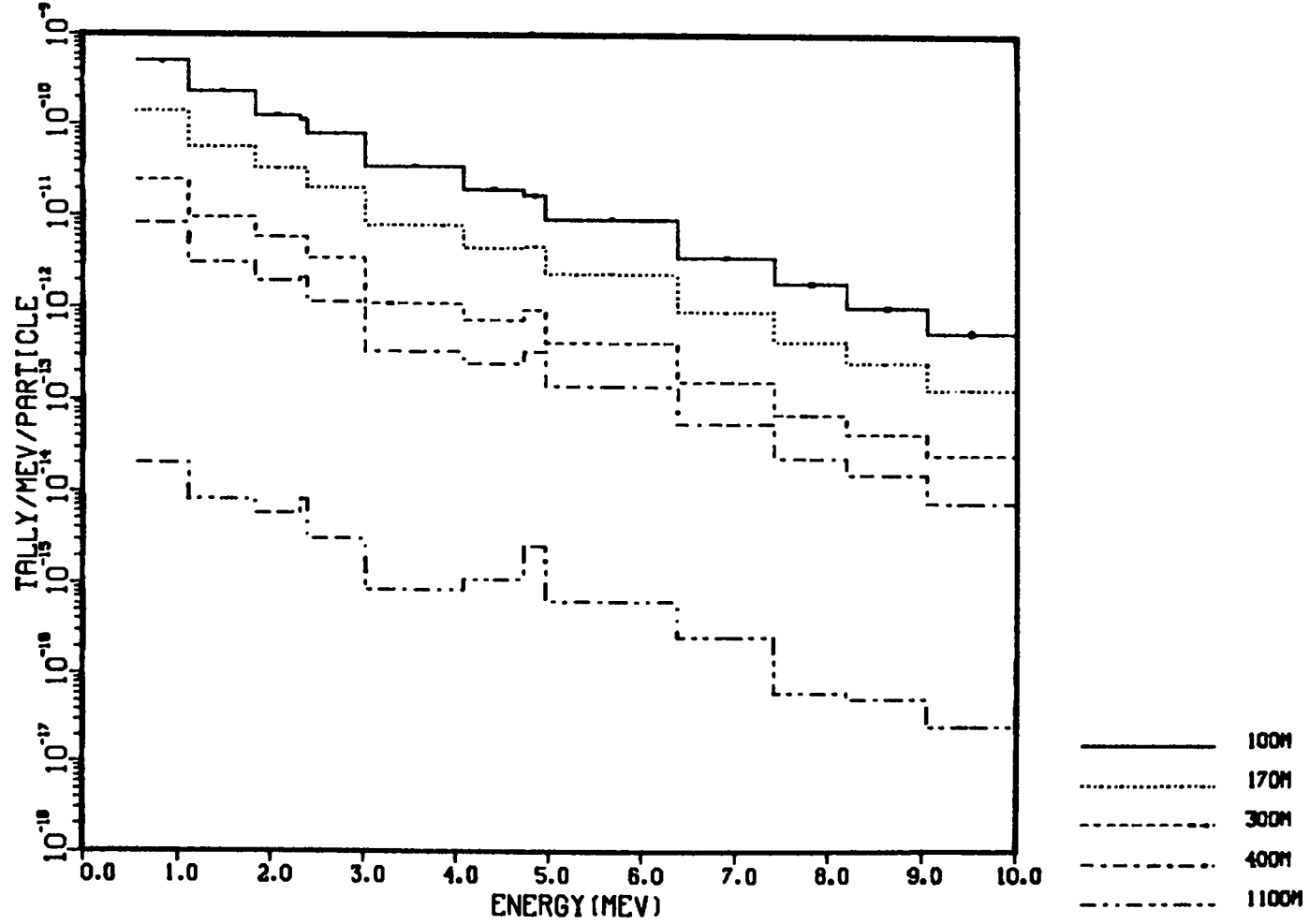


Fig. 4. Neutron flux at 100, 170, 300, 400, and 1100 m.

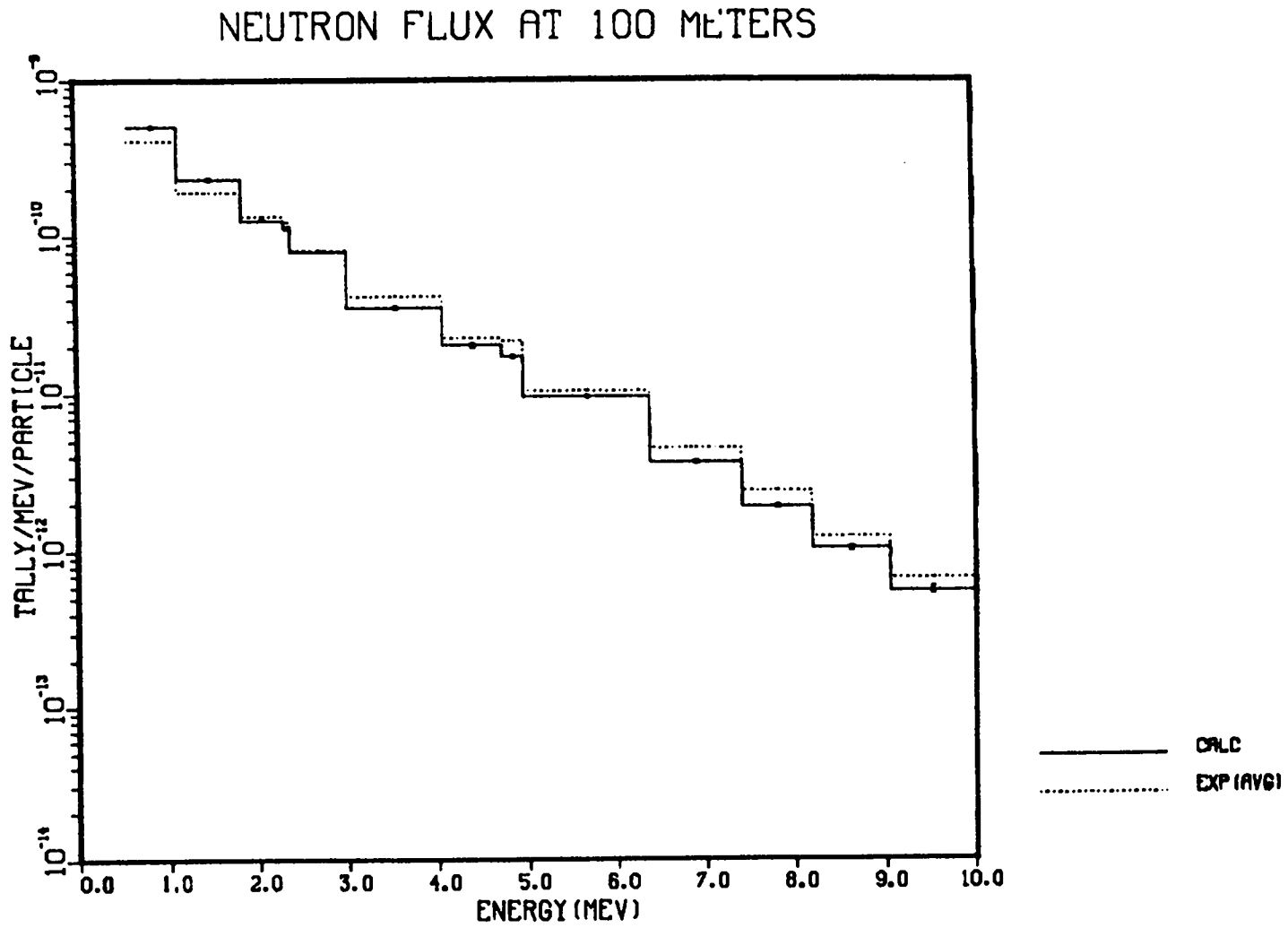


Fig. 5. Neutron flux at 100 m compared to averaged experimental values.

NEUTRON FLUX AT 170 METERS

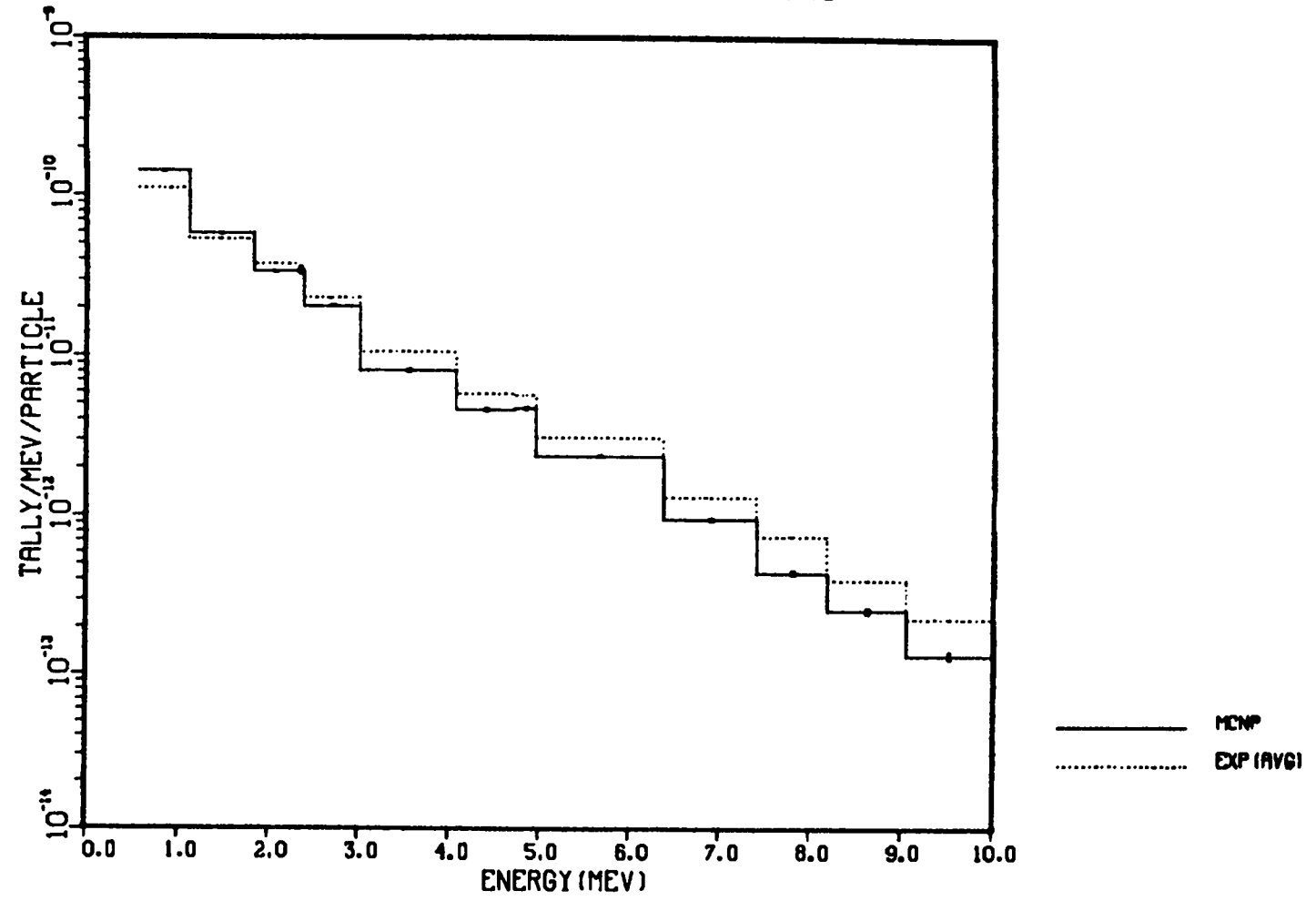


Fig. 6. Neutron flux at 170 m compared to averaged experimental values.

NEUTRON FLUX AT 300 METERS

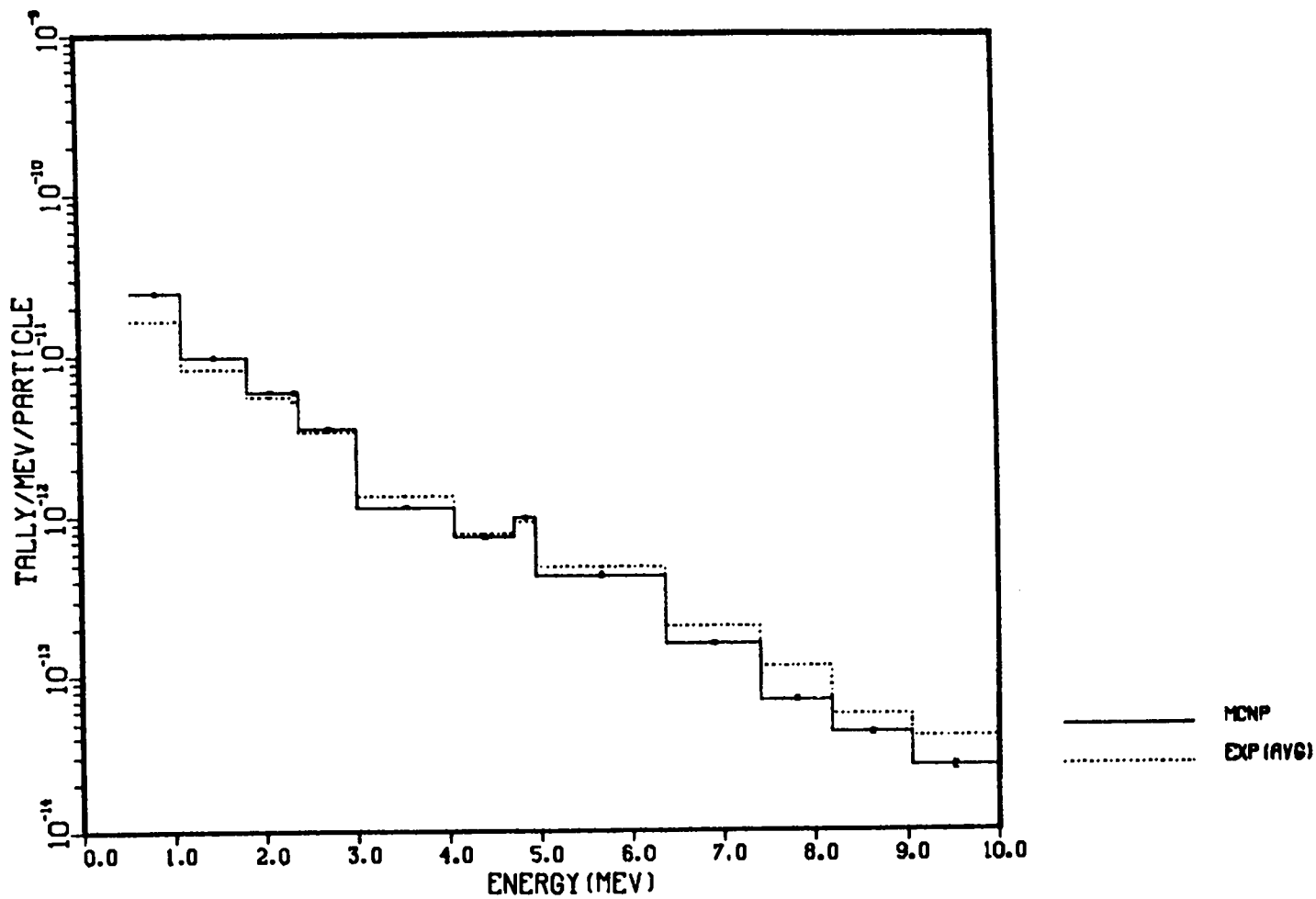


Fig. 7. Neutron flux at 300 m compared to averaged experimental values.

NEUTRON FLUX AT 400 METERS

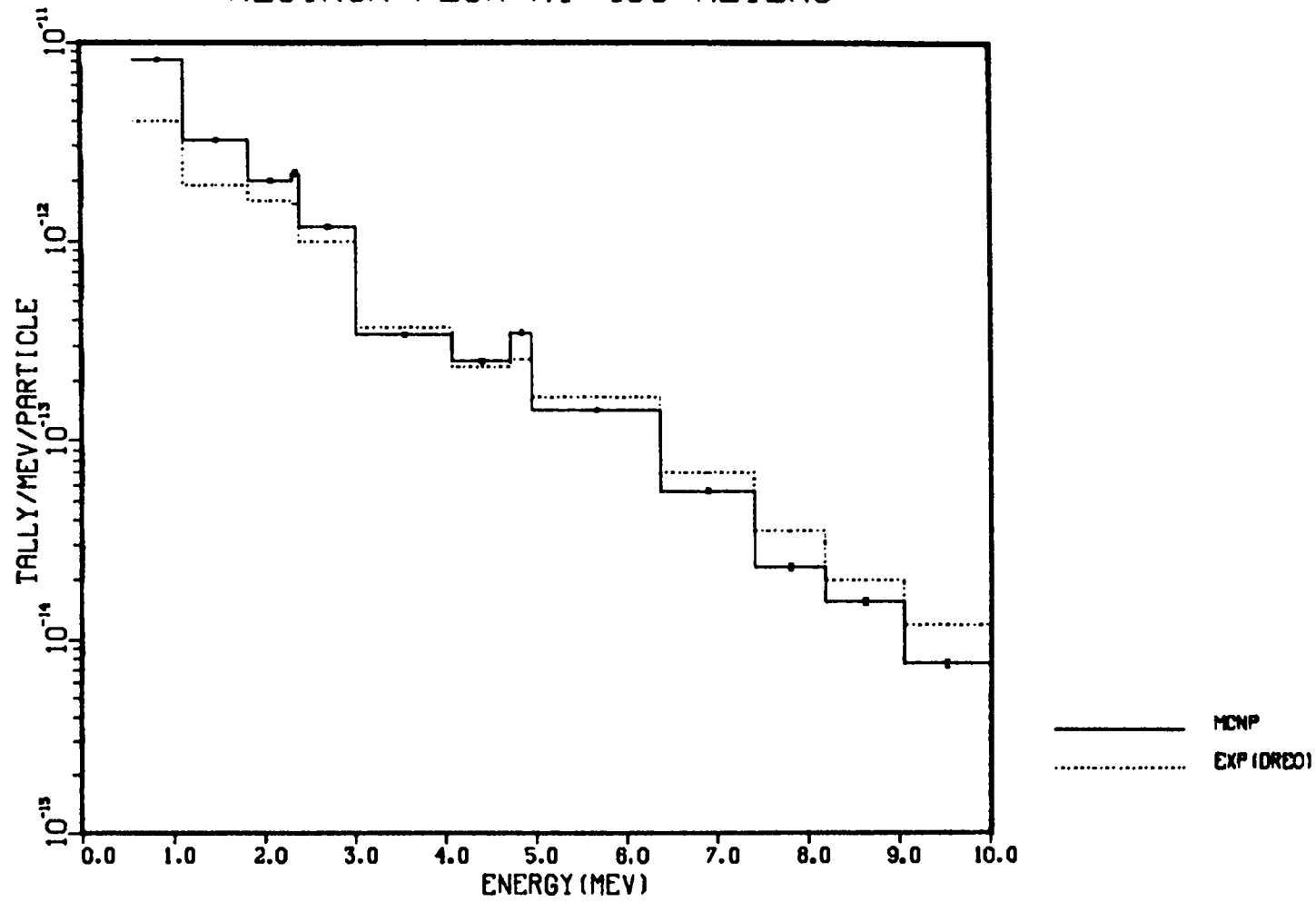


Fig. 8. Neutron flux at 400 m compared to DREO measured values.

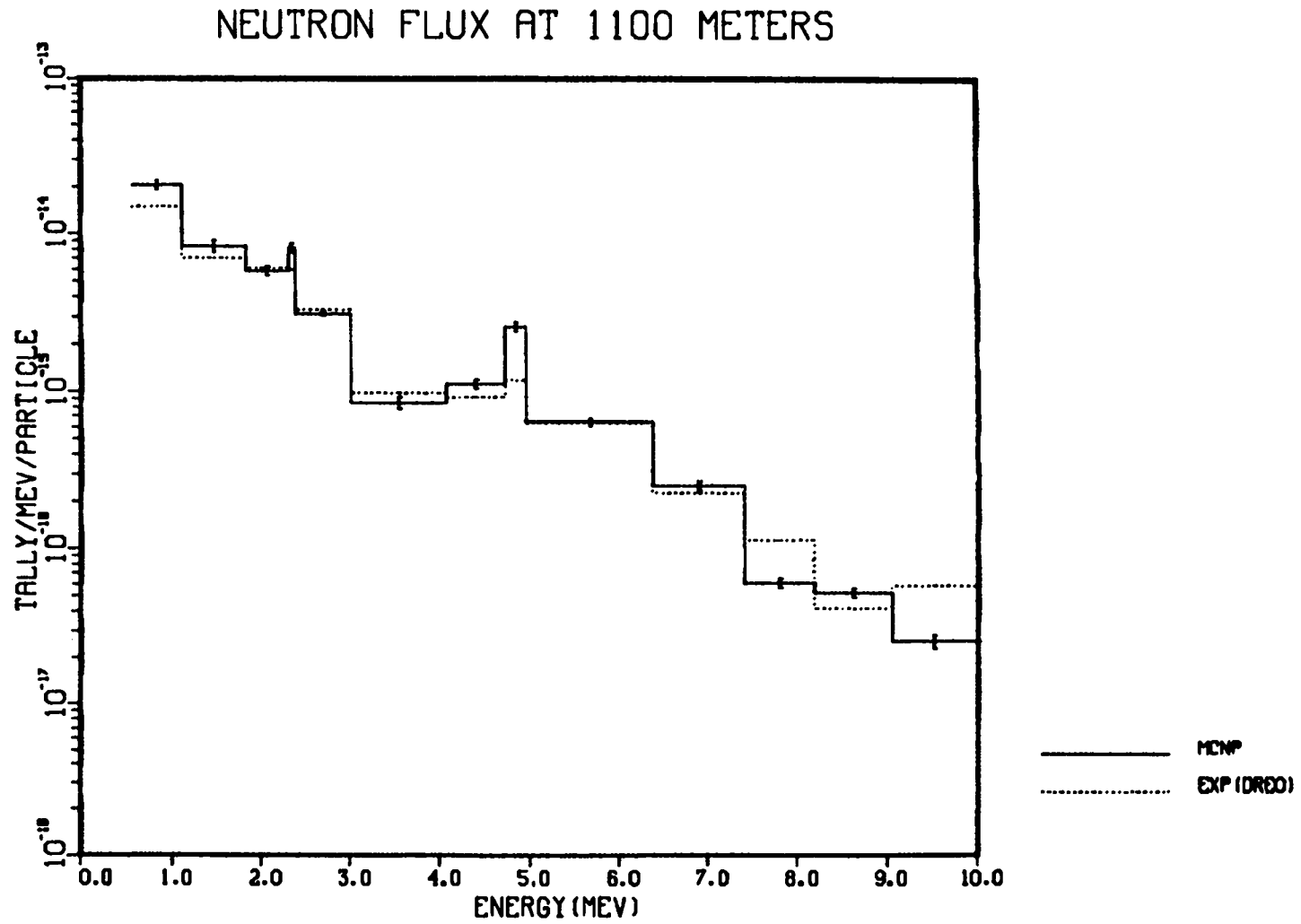


Fig. 9. Neutron flux at 1100 m compared to DREO measured values.

APRD REACTOR NEUTRON SPECTRUM MEASUREMENTS

CALCULATIONS VS. EXPERIMENT AVERAGE

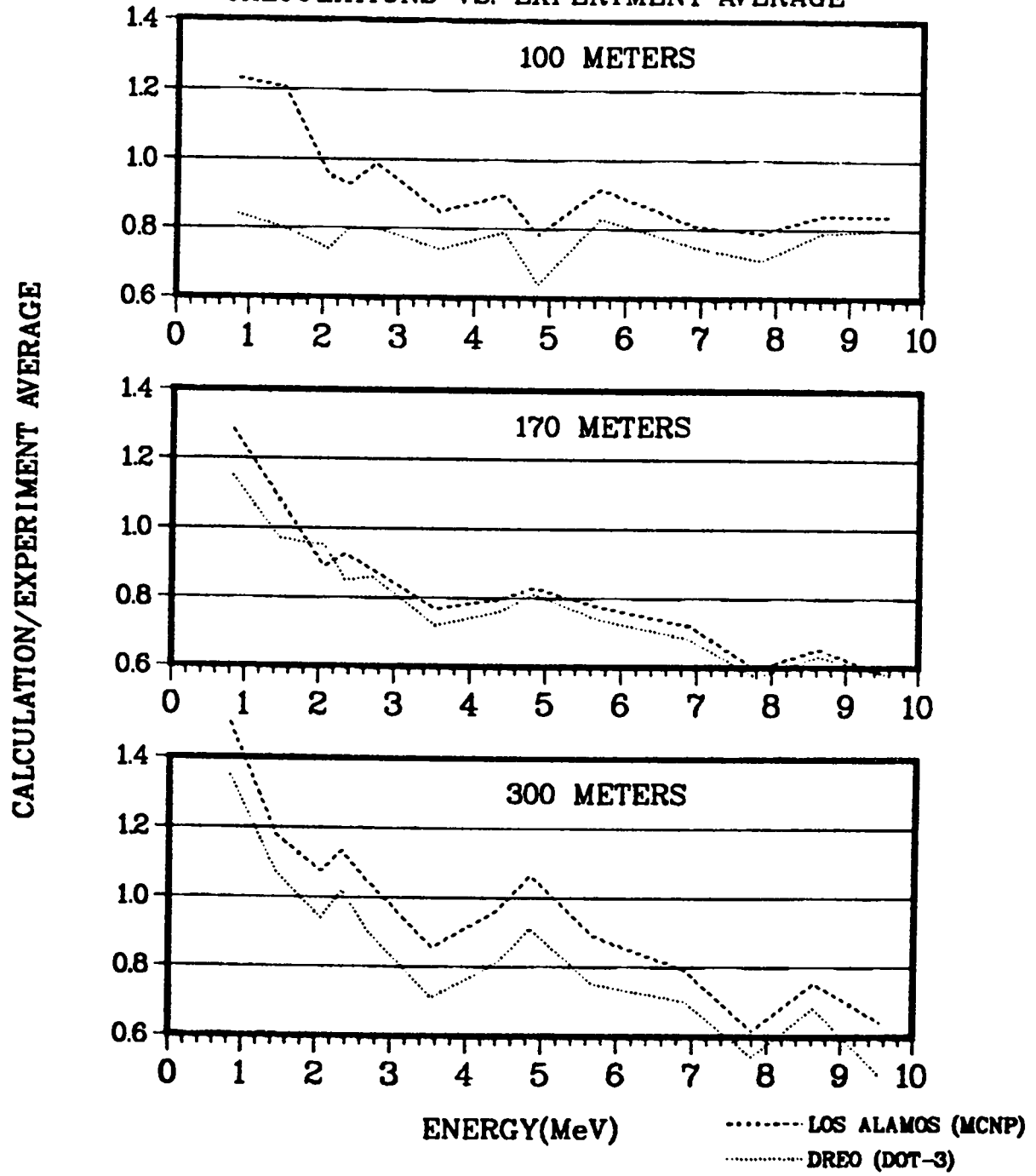


Fig. 10. Calculated neutron spectrum divided by experimental average at 100, 170, and 300 m.

APRD REACTOR NEUTRON SPECTRUM MEASUREMENTS CALCULATIONS VS. DREO EXPERIMENT

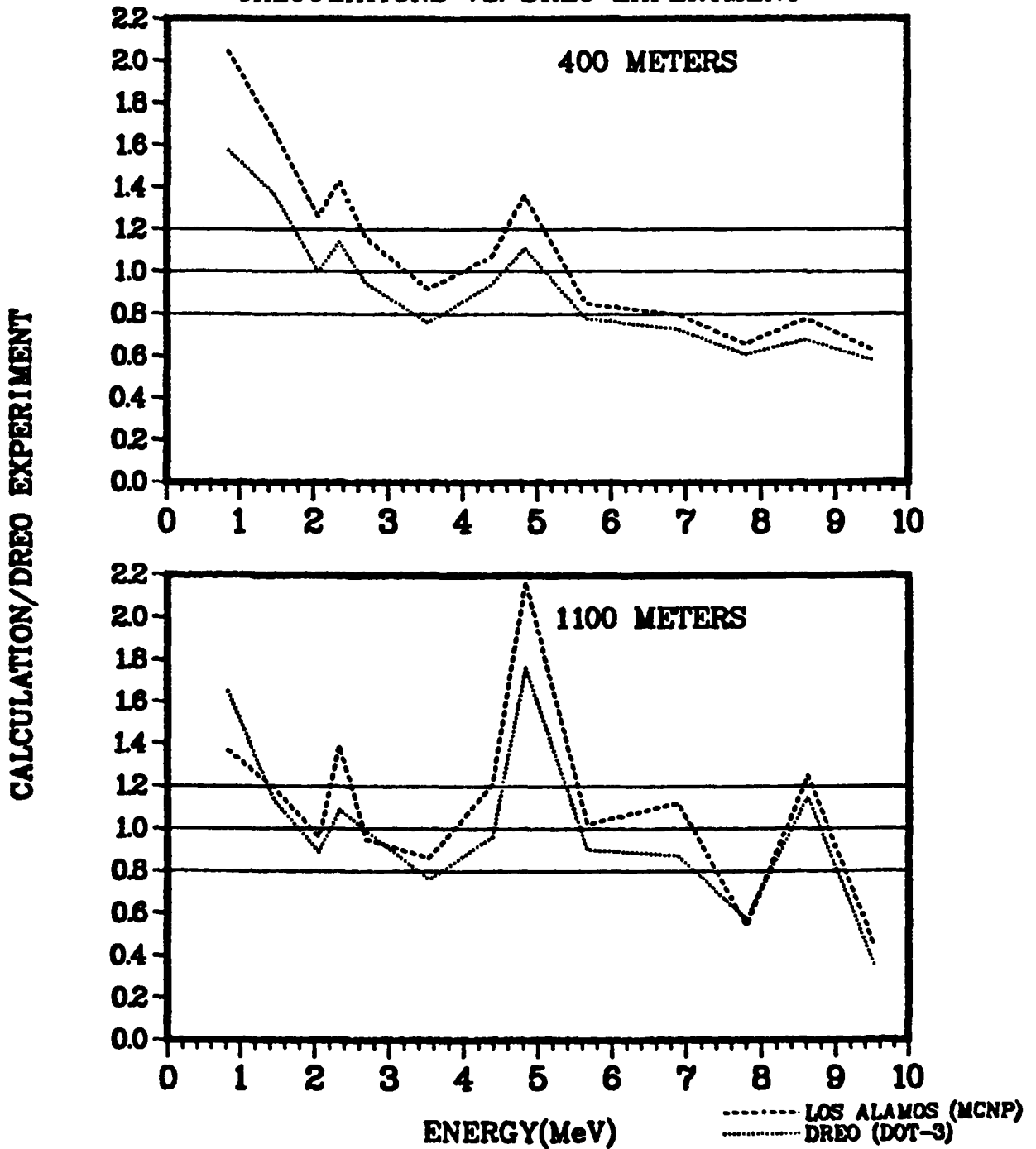


Fig. 11. Calculated neutron spectrum divided by DREO measured values at 400 and 1100 m.

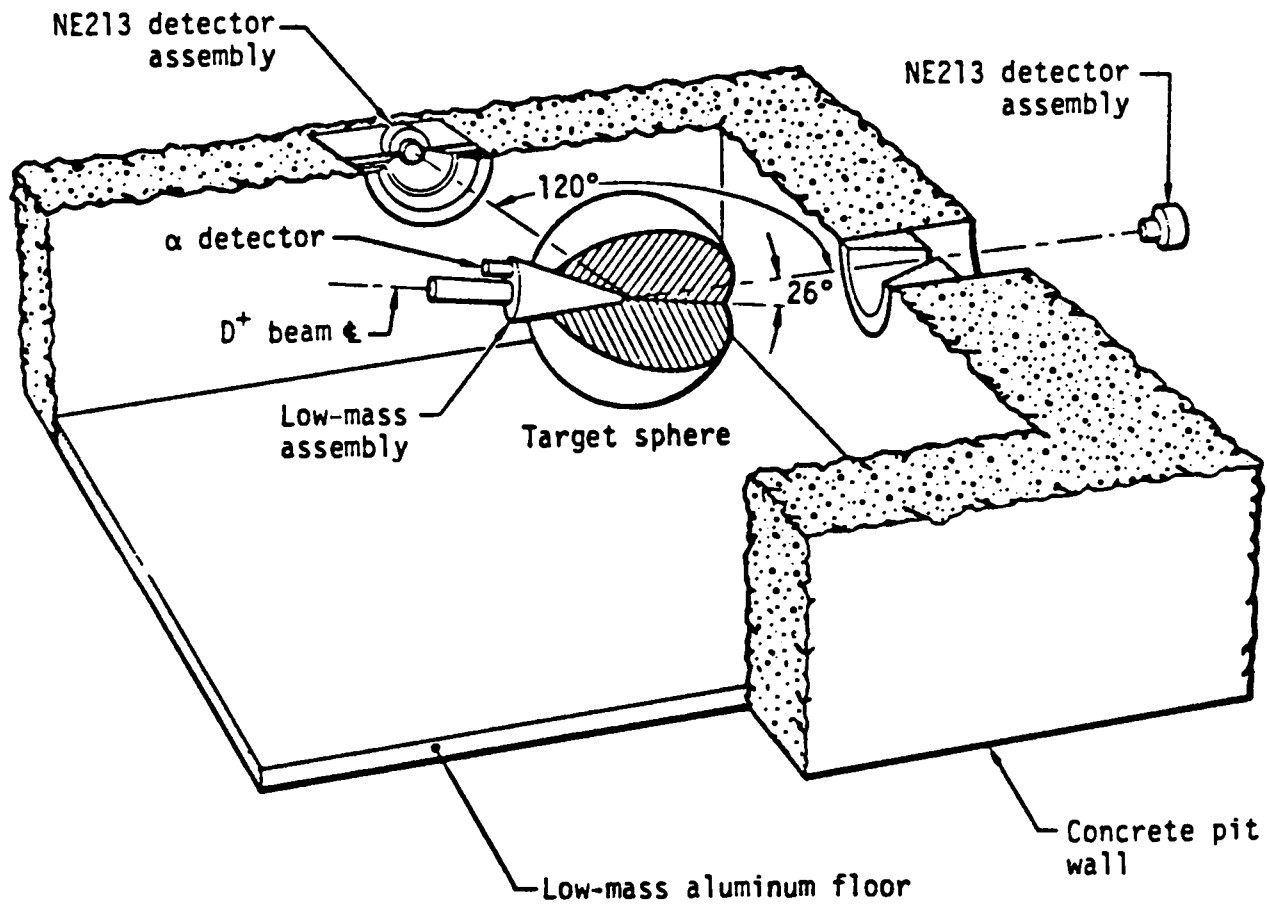


Fig. 12. Time-of-flight geometry of the target sphere and collimated neutron detector in Livermore pulsed sphere experiments.

LIQ. OXYGEN, ENDF5

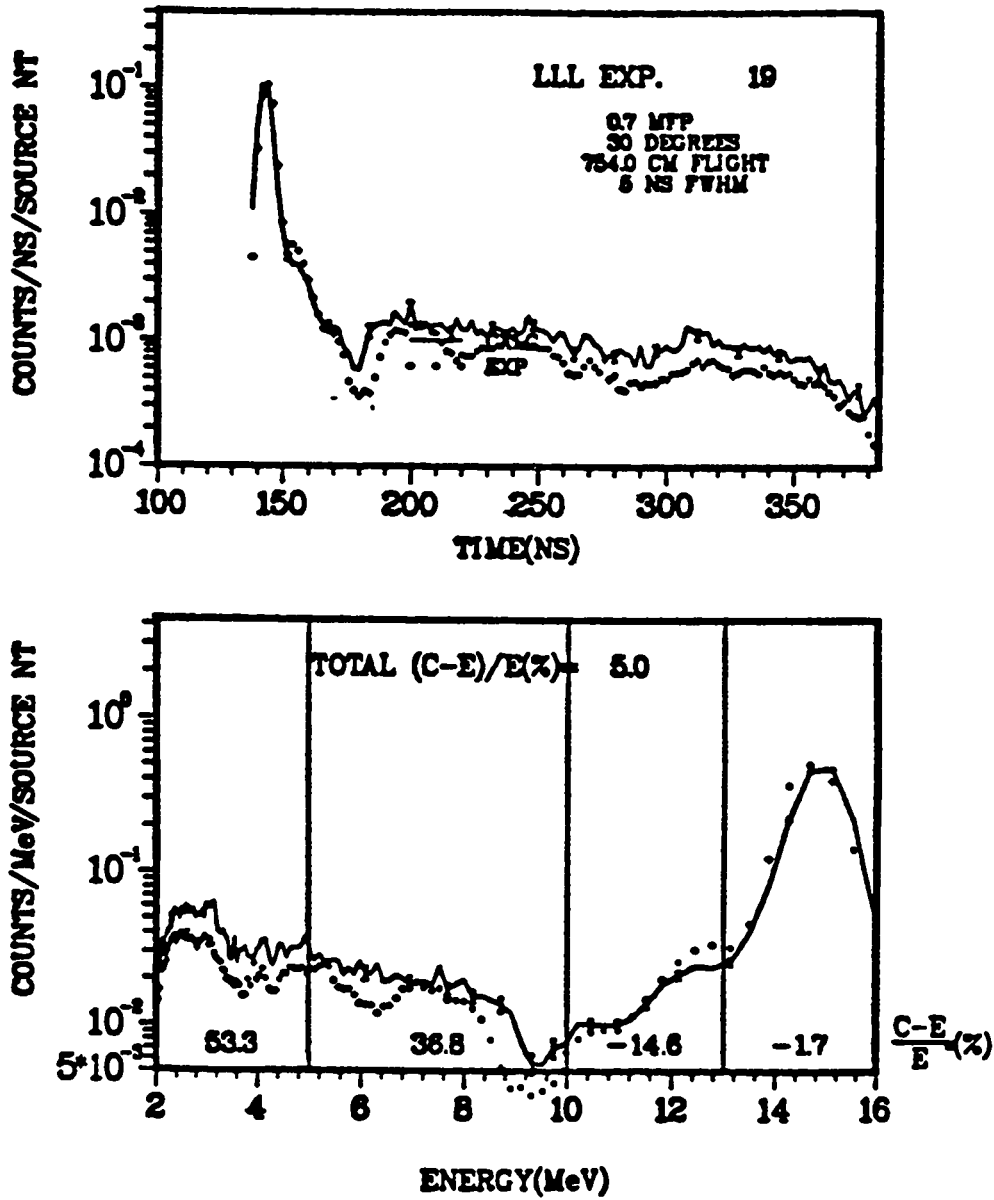


Fig. 13. Pulsed sphere results for liquid oxygen -- experiment versus ENDF/B-V calculation.

LIQ. NITROGEN, ENDF5

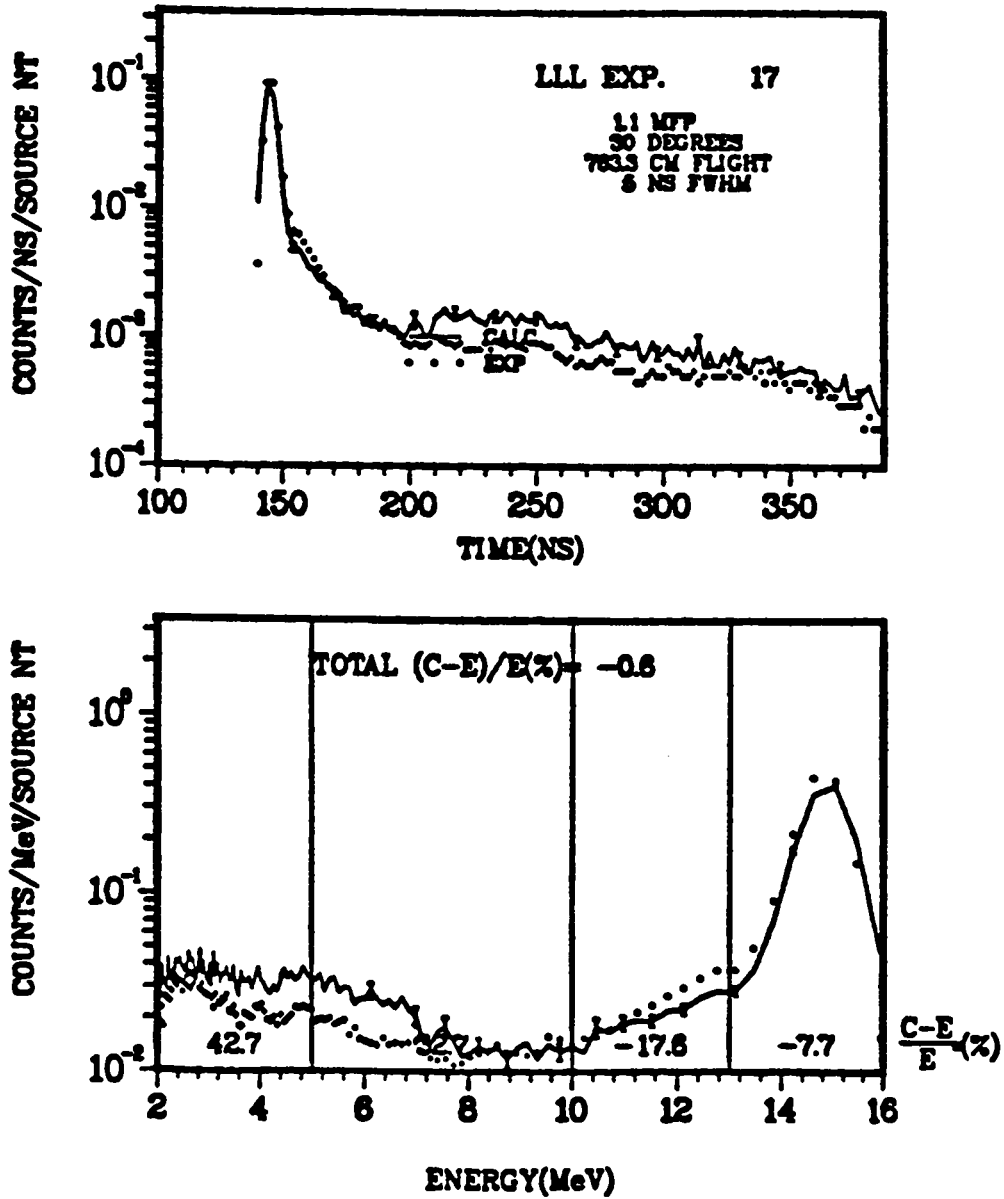


Fig. 14. Pulsed sphere results for liquid nitrogen (1.1 mfp) — experiment versus ENDF/B-V calculation.

LIQ. NITROGEN, ENDF5

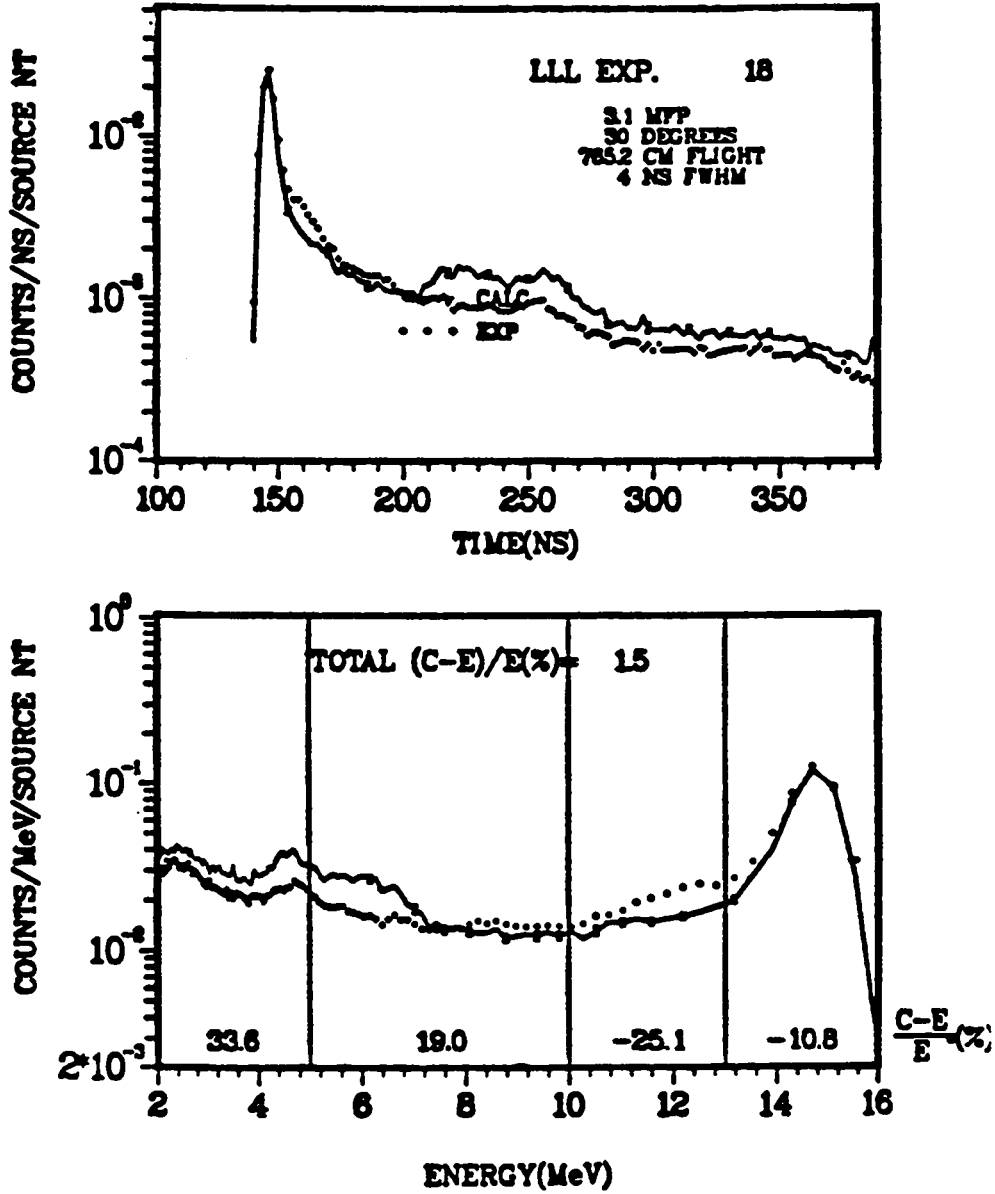


Fig. 15. Pulsed sphere results for liquid nitrogen (3.1 mfp) — experiment versus ENDF/B-V calculation.

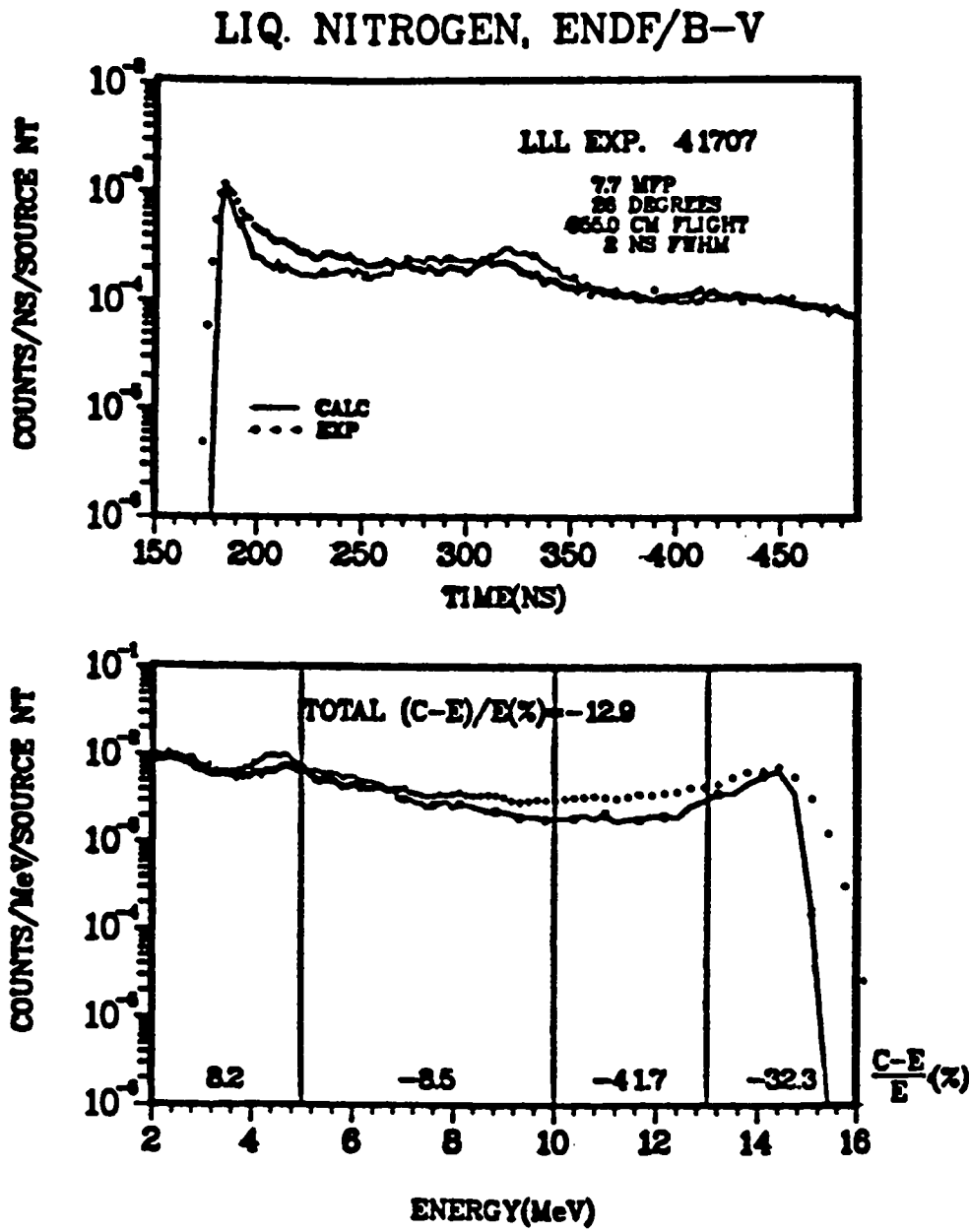


Fig. 16. Pulsed sphere results for liquid nitrogen (7.7 mfp) -- experiment versus ENDF/B-V calculation.

WATER, ENDF5

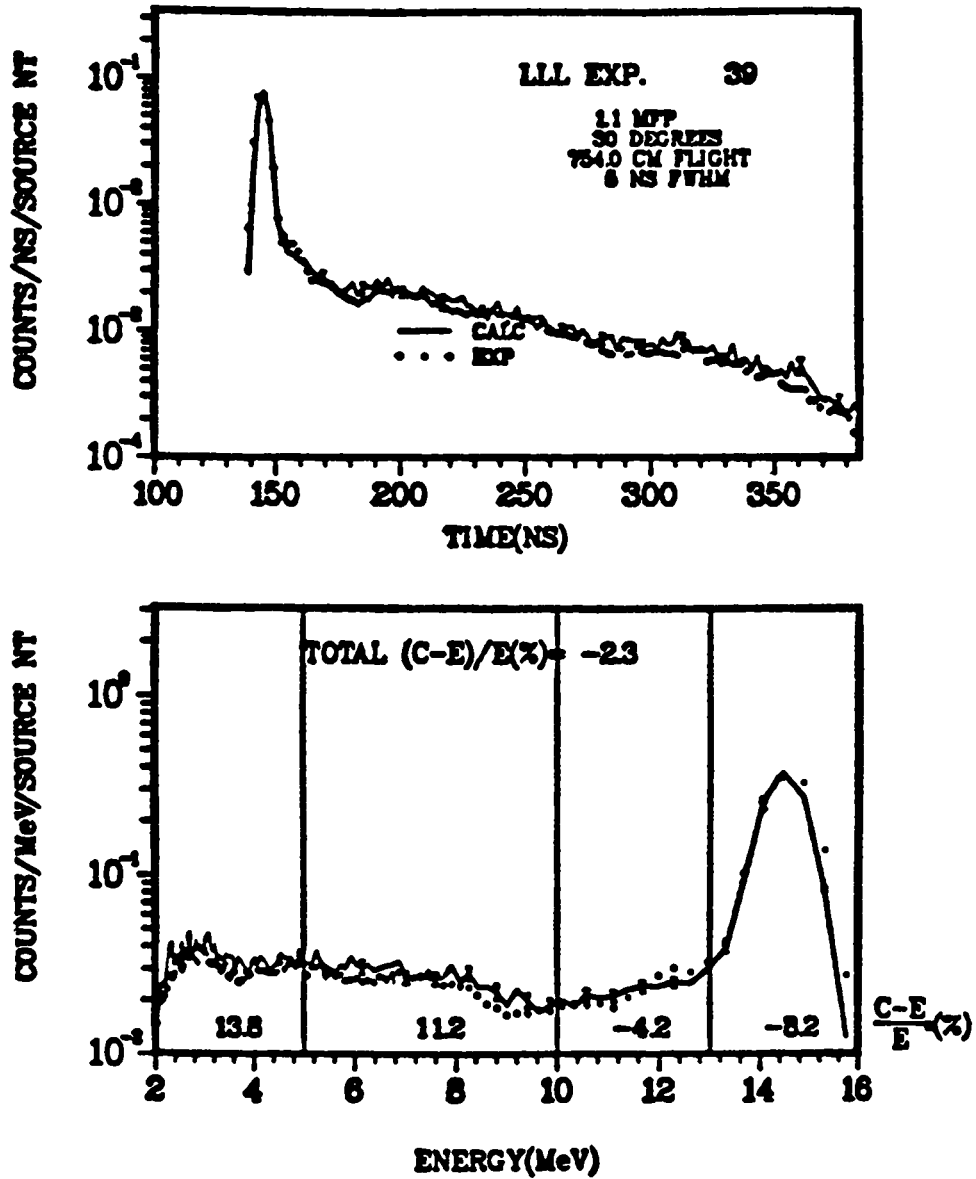


Fig. 17. Pulsed sphere results for water (1.1 mfp) — experiment versus ENDF/B-V calculation.

WATER, ENDF5

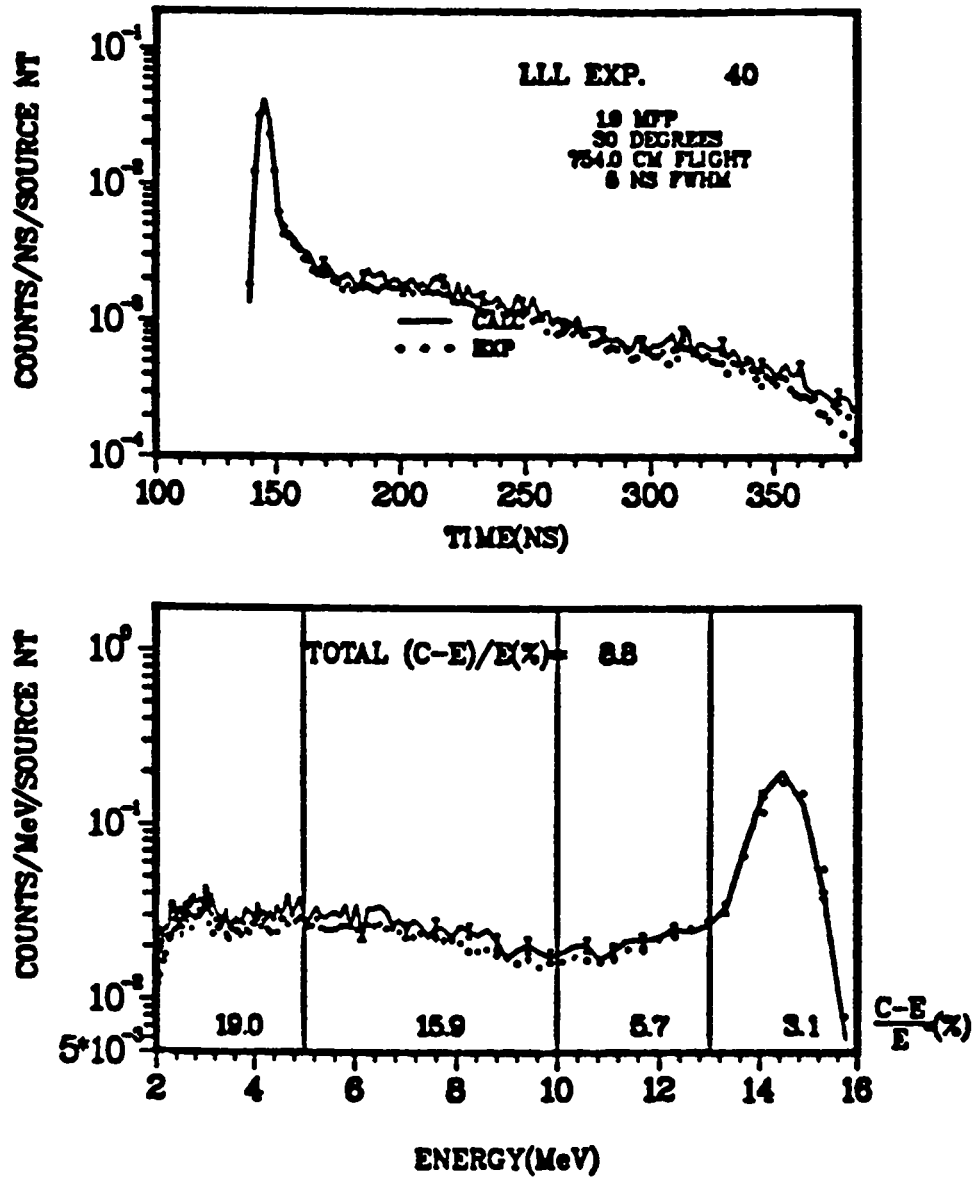
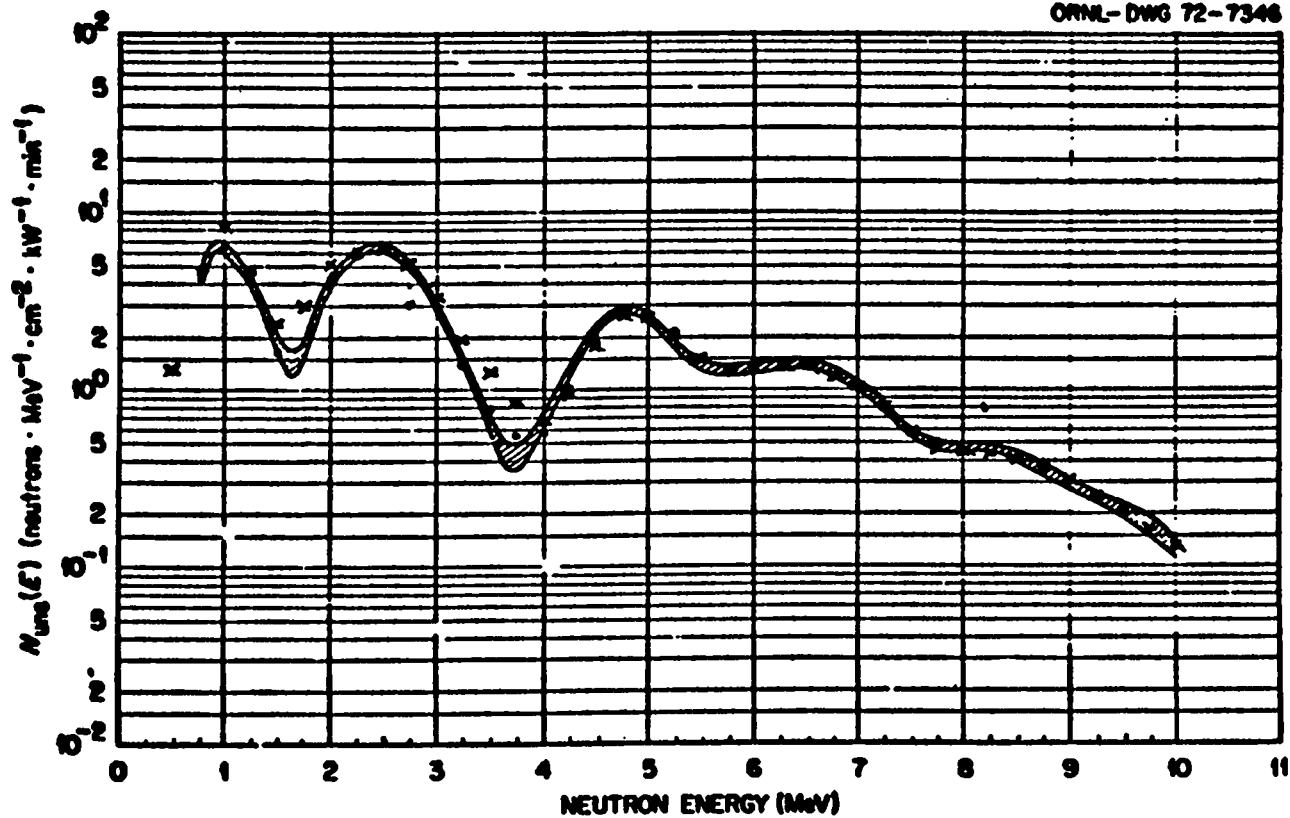


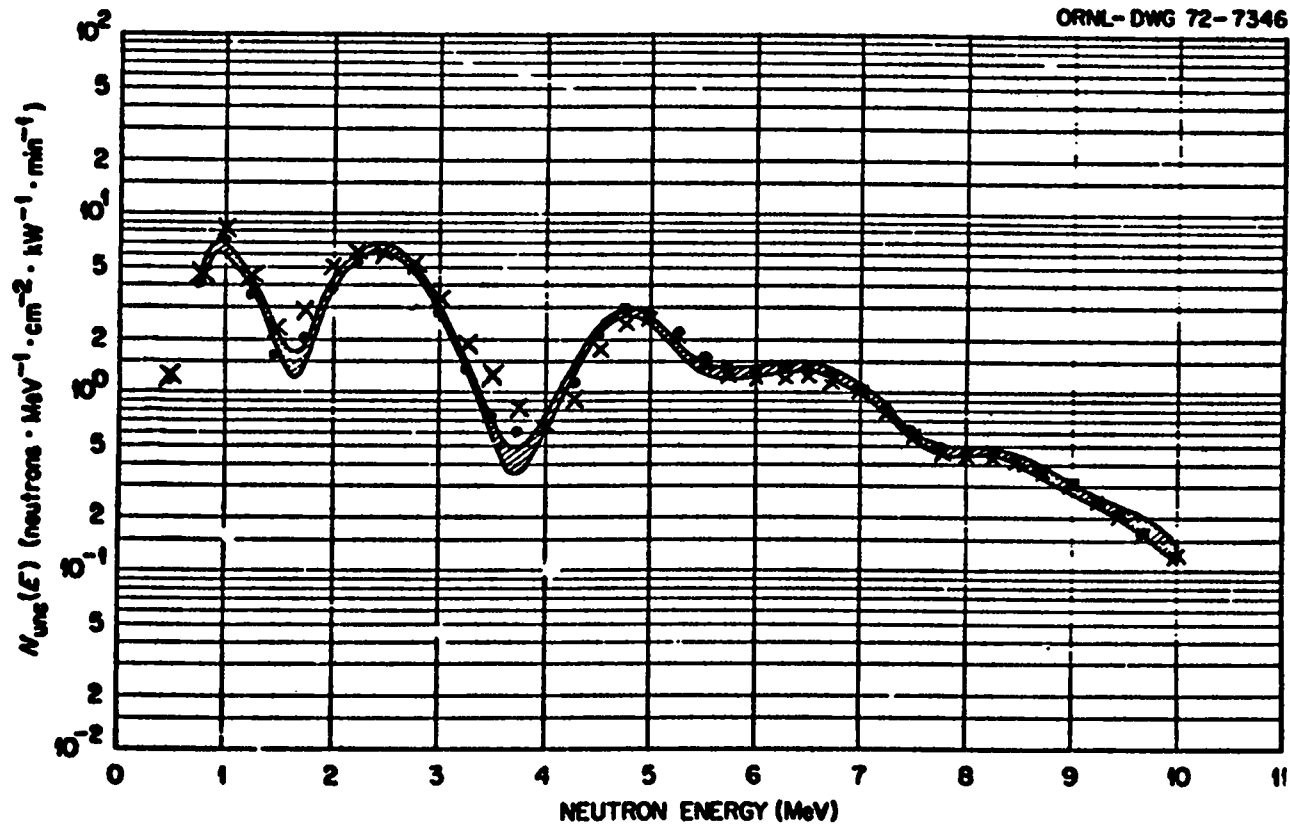
Fig. 18. Pulsed sphere results for water (1.9 mfp) — experiment versus ENDF/B-V calculation.



Transmitted Spectrum Through Nitrogen.

- X ENDF/B-V ZAID=7014.50
- MODIFIED (N14F) ZAID=7014.73

Fig. 19. Transmitted spectrum through nitrogen broomstick with calculations from ENDF/B-V and N14F modified cross sections.



Transmitted Spectrum Through Nitrogen.

- × ENDF/B-V ZAIID=7014.50
- MODIFIED (N14FF) ZAIID=7014.86

Fig. 20. Transmitted spectrum through nitrogen broomstick with calculations from ENDF/B-V and N14FF modified cross sections.

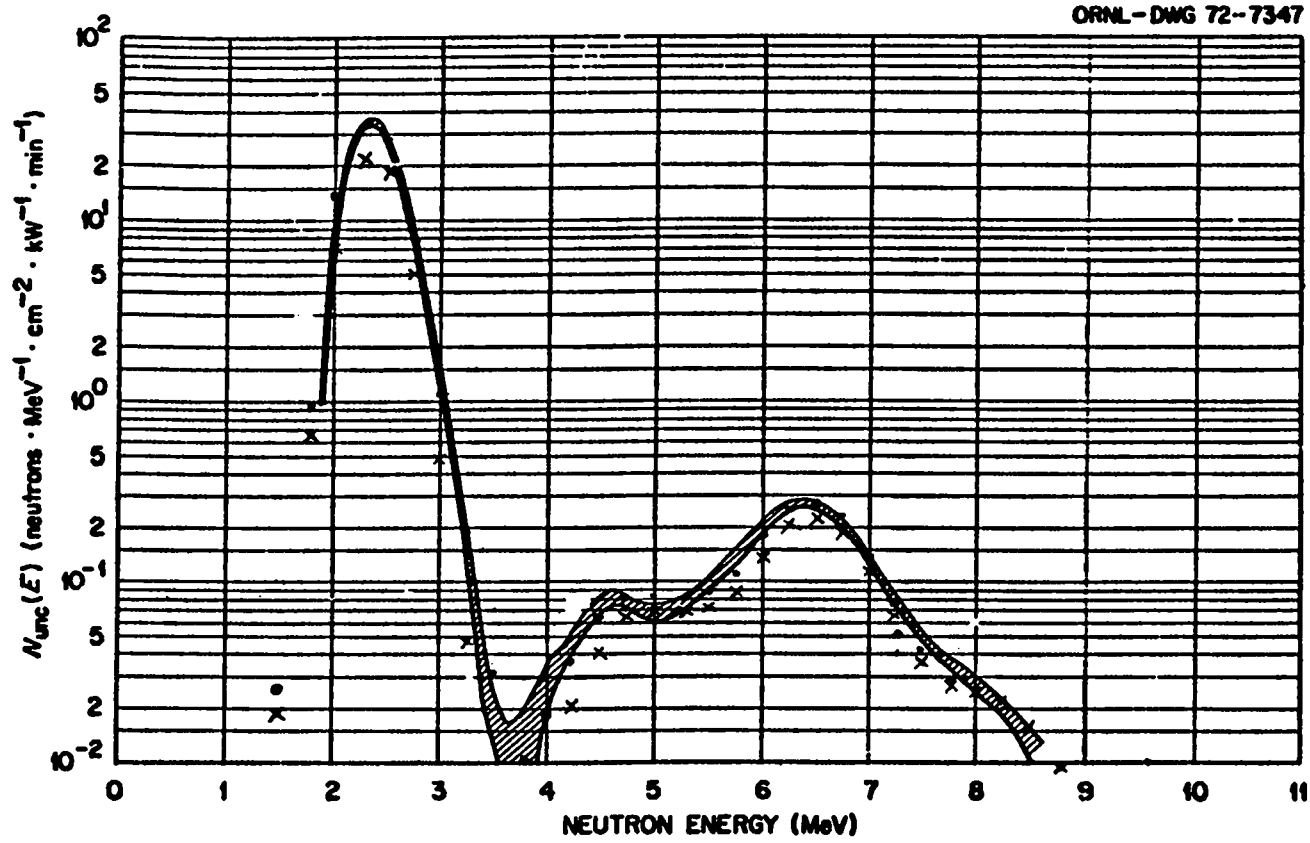


Fig. 2. Transmitted Spectrum Through Oxygen.

- X ENDF/B-V ZAID=8016.50
- MODIFIED (O16F) ZAID=8016.73

Fig. 21. Transmitted spectrum through oxygen broomstick with calculations from ENDF/B-V and O16F modified cross sections.

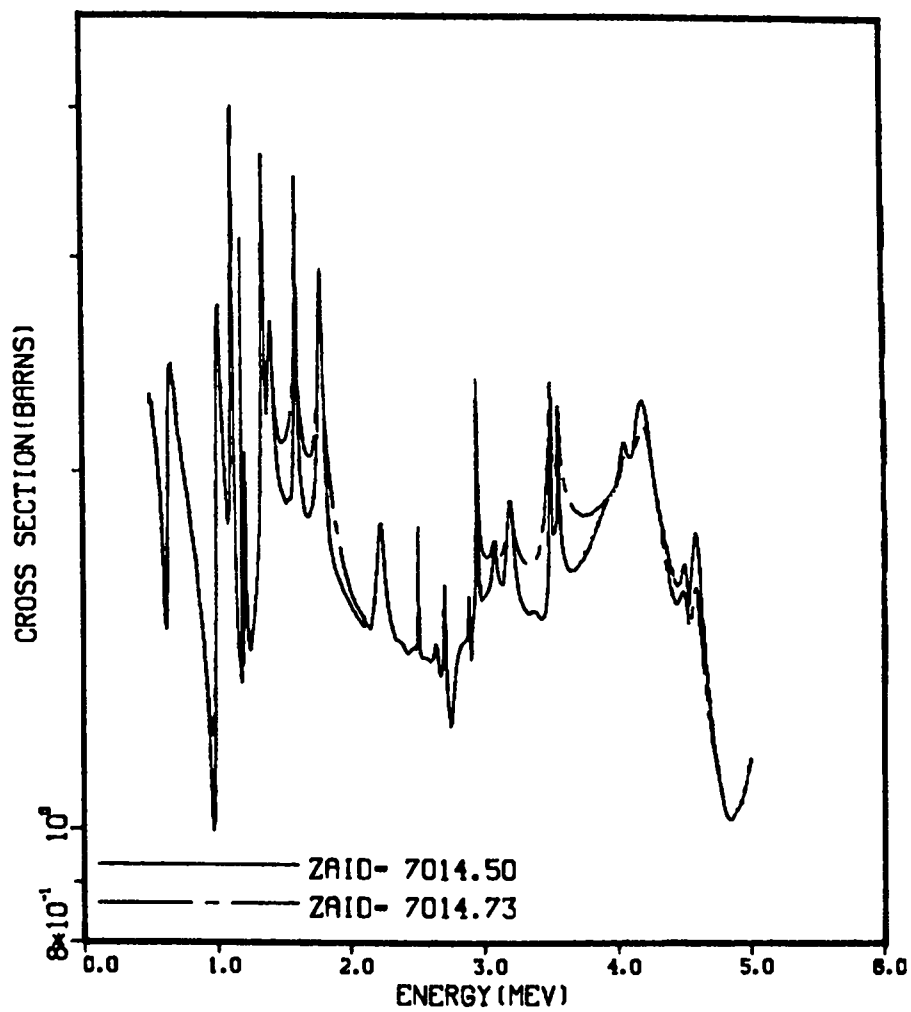


Fig. 22. Modified N-14 total cross section (Zaid=7014.73) compared with ENDF/B-V (ZAID=7014.50).

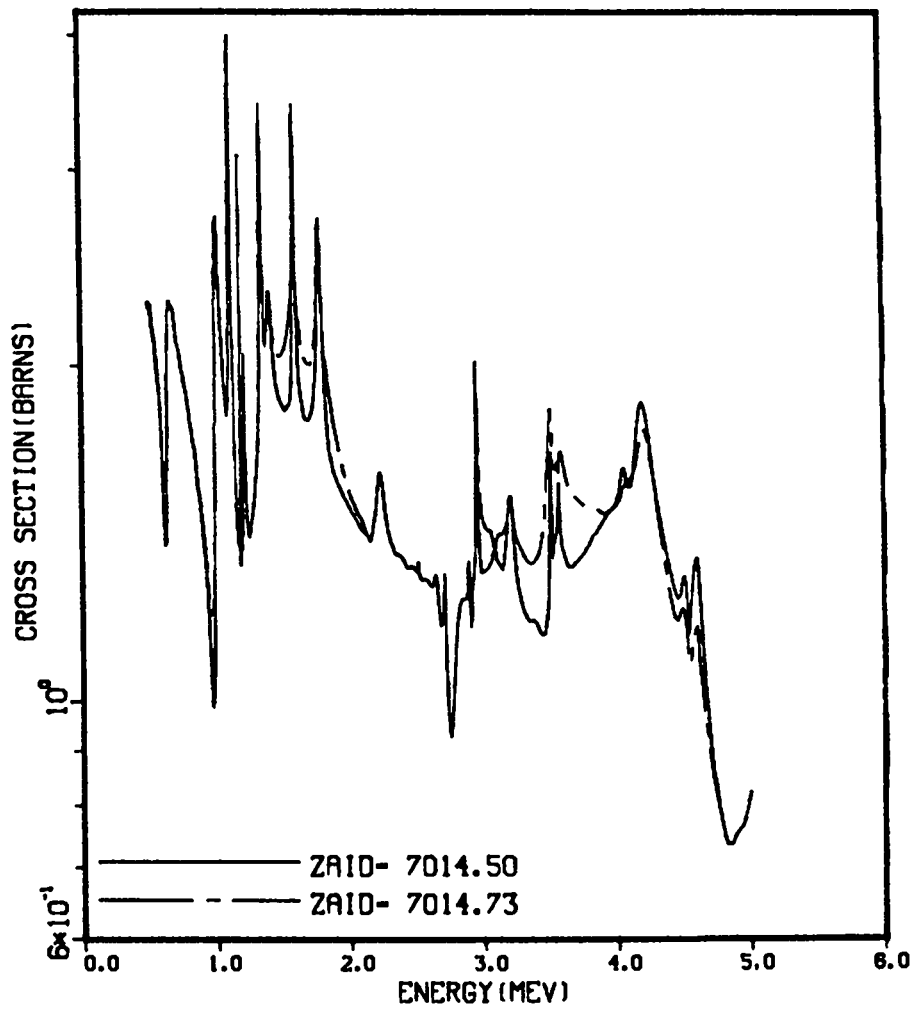


Fig. 23. Modified N-14 elastic cross section (ZAID=7014.73) compared with ENDF/B-V (ZAID=7014.50).

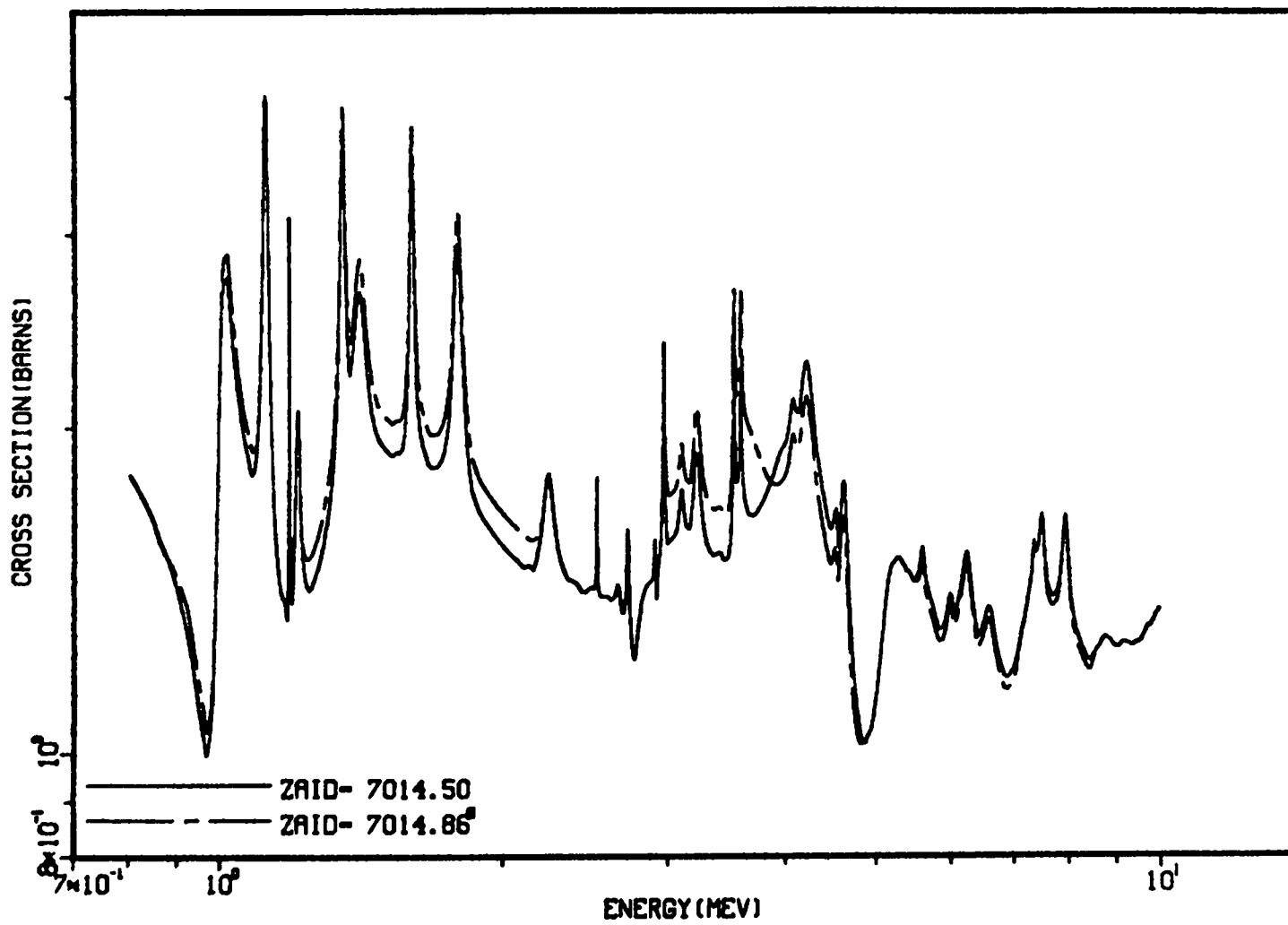


Fig. 24. Modified N-14 total cross section (ZAID=7014.86) compared with ENDF/B-V (ZAID=7014.50).

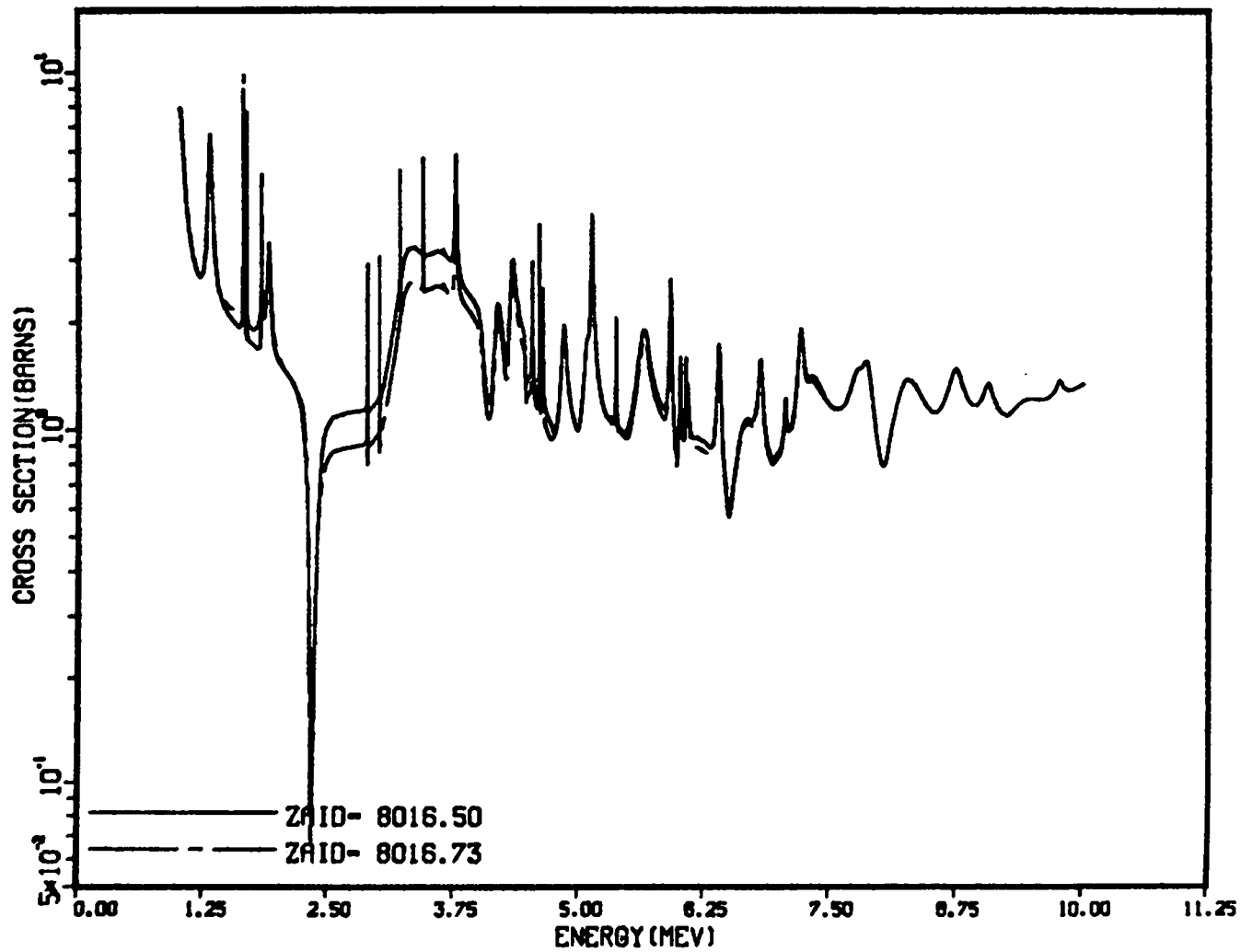


Fig. 25. Modified 0-16 total cross section (ZAID=8016.73) compared with ENDF/B-V (ZAID=8016.50).

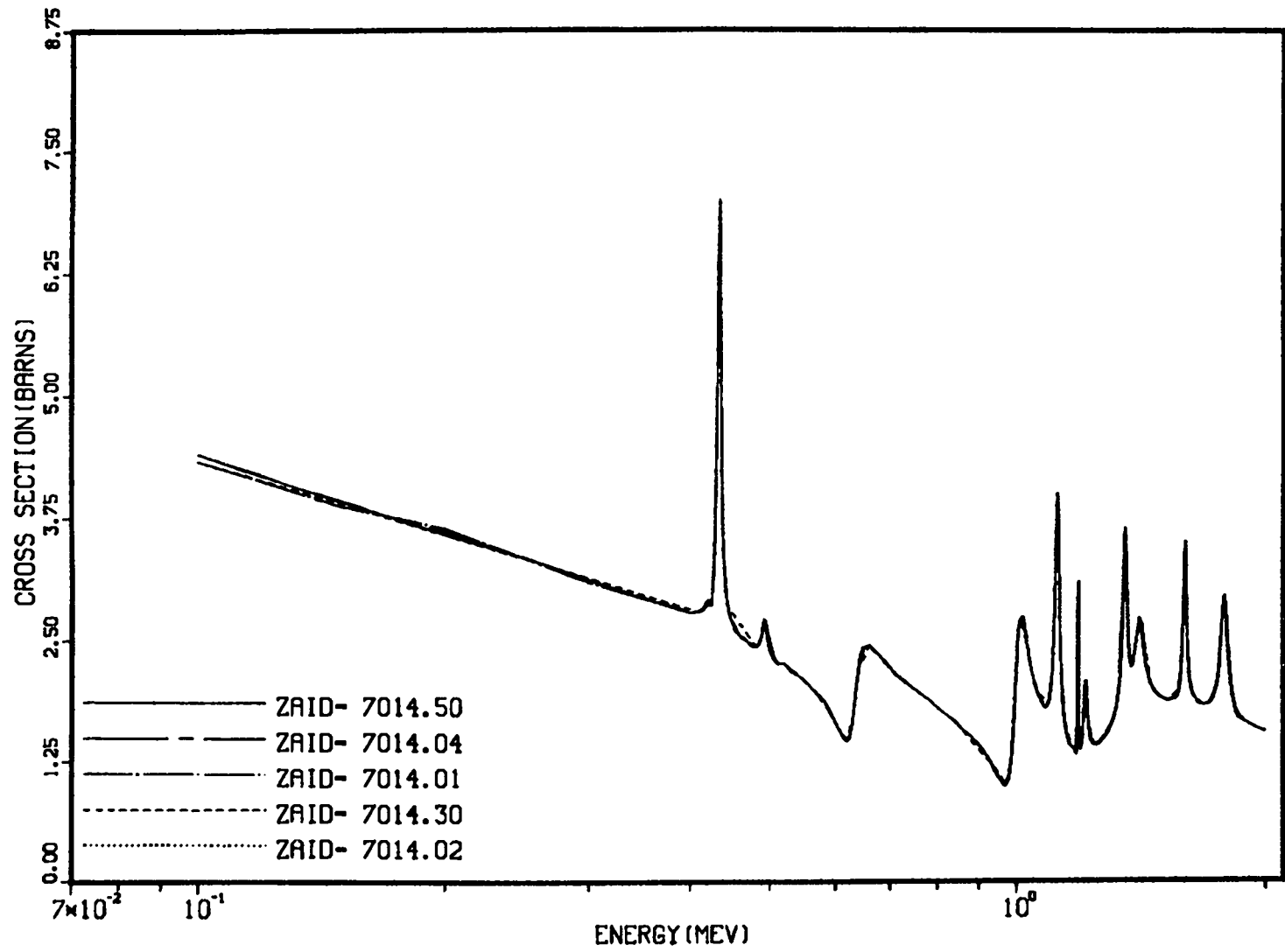


Fig. 26. Total cross section for five different nitrogen evaluations.

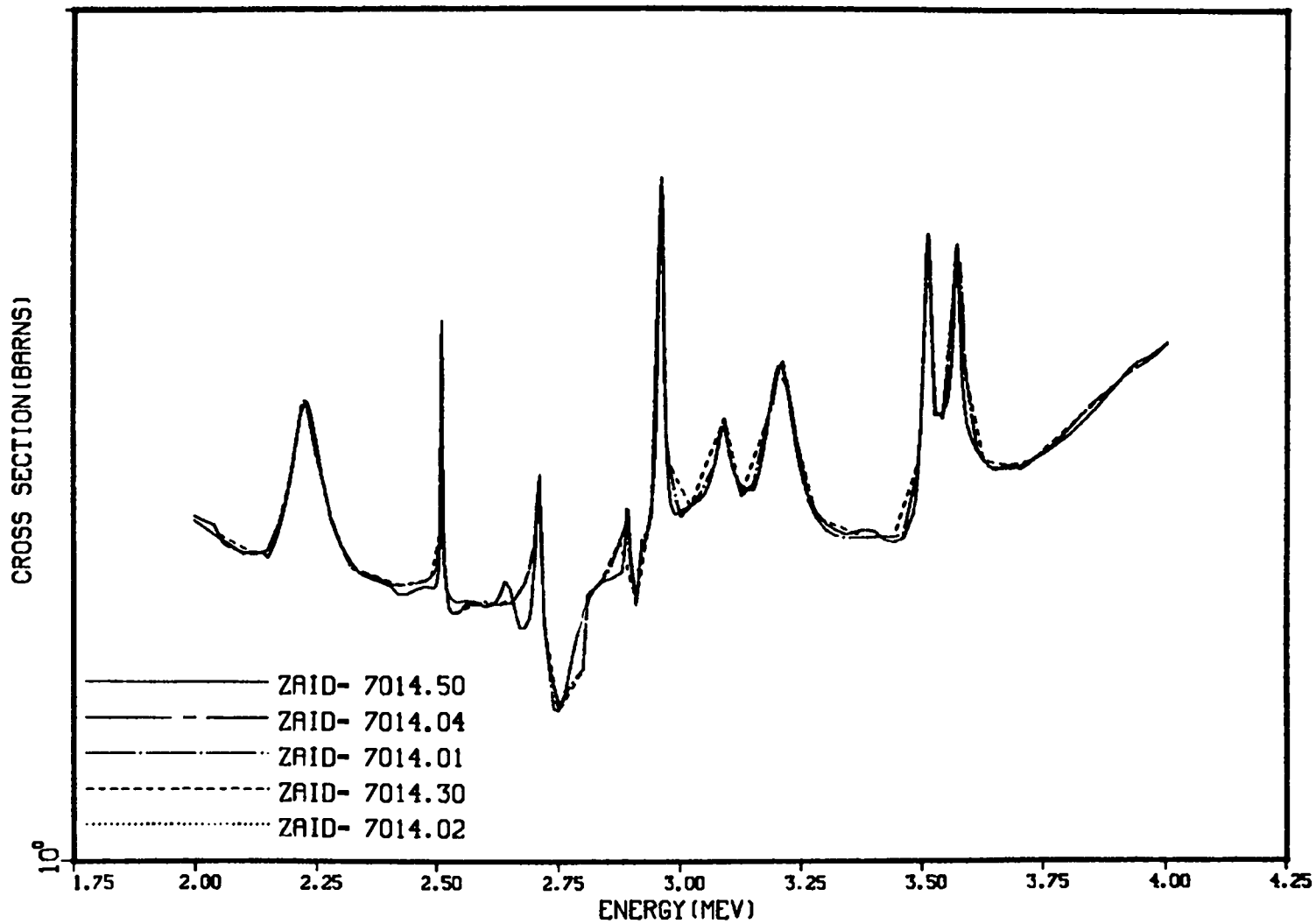


Fig. 27. Total cross section for five different nitrogen evaluations (expanded scale).

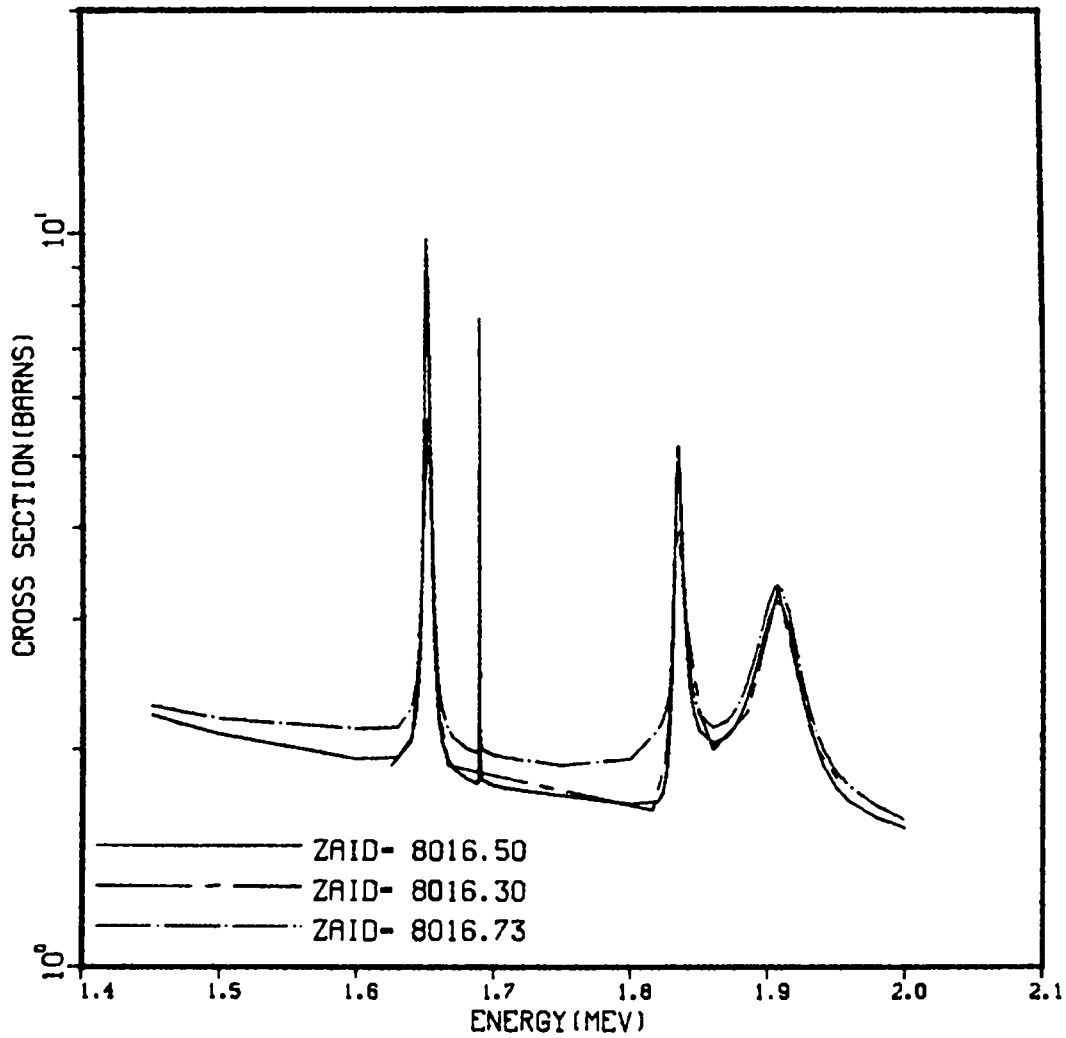


Fig. 28. Total 0-16 cross section from ENDF/B-V (ZAID=8016.50), ENDL-76 (ZAID=8016.30), and modified (ZAID=8016.73).

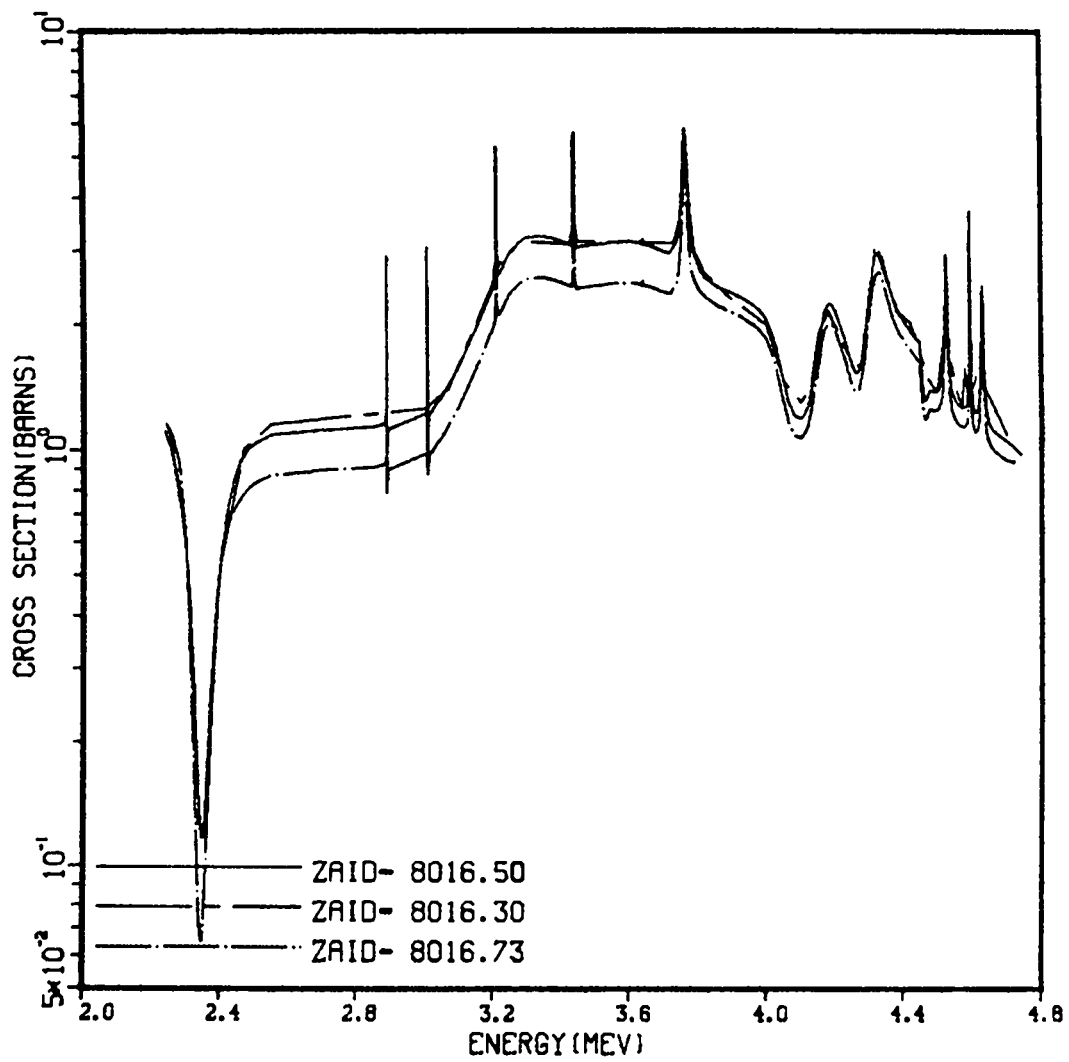
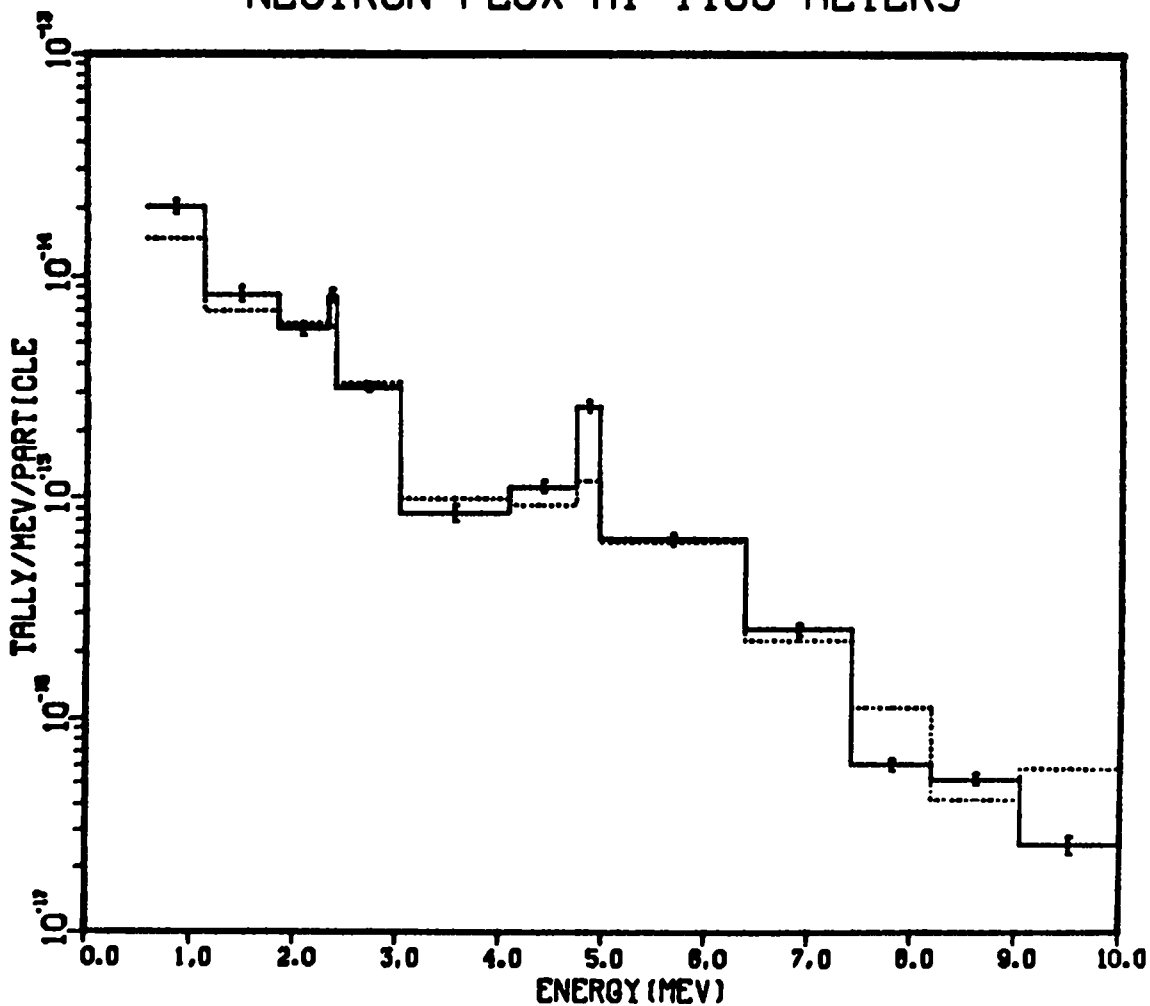


Fig. 29. Total 0-16 cross section from ENDF/B-V (ZAID=8016.50), ENDL-76 (ZAID=8016.30), and modified (ZAID=8016.73) (expanded scale).

NEUTRON FLUX AT 1100 METERS



```

MCNP      20      09/03/81
T         09/10/81 19:51:53
TALLY=    5
NEUTRON
NPS      300000
BIN NORMED
RUNTIME=  ENDF/B-V
DETECTOR  1
FLAG/DIR  1
USR       1
SEGMENT   1
MULT      1
COSINE    1
ENERGY    *
TIME      1
DUMP      5
-----  ENDF/B-V
.....  EXPERIMENT
    
```

Fig. 30. Neutron flux at 1100 m calculated using ENDF/B-V compared with DREO experiment.

NEUTRON FLUX AT 1100 METERS

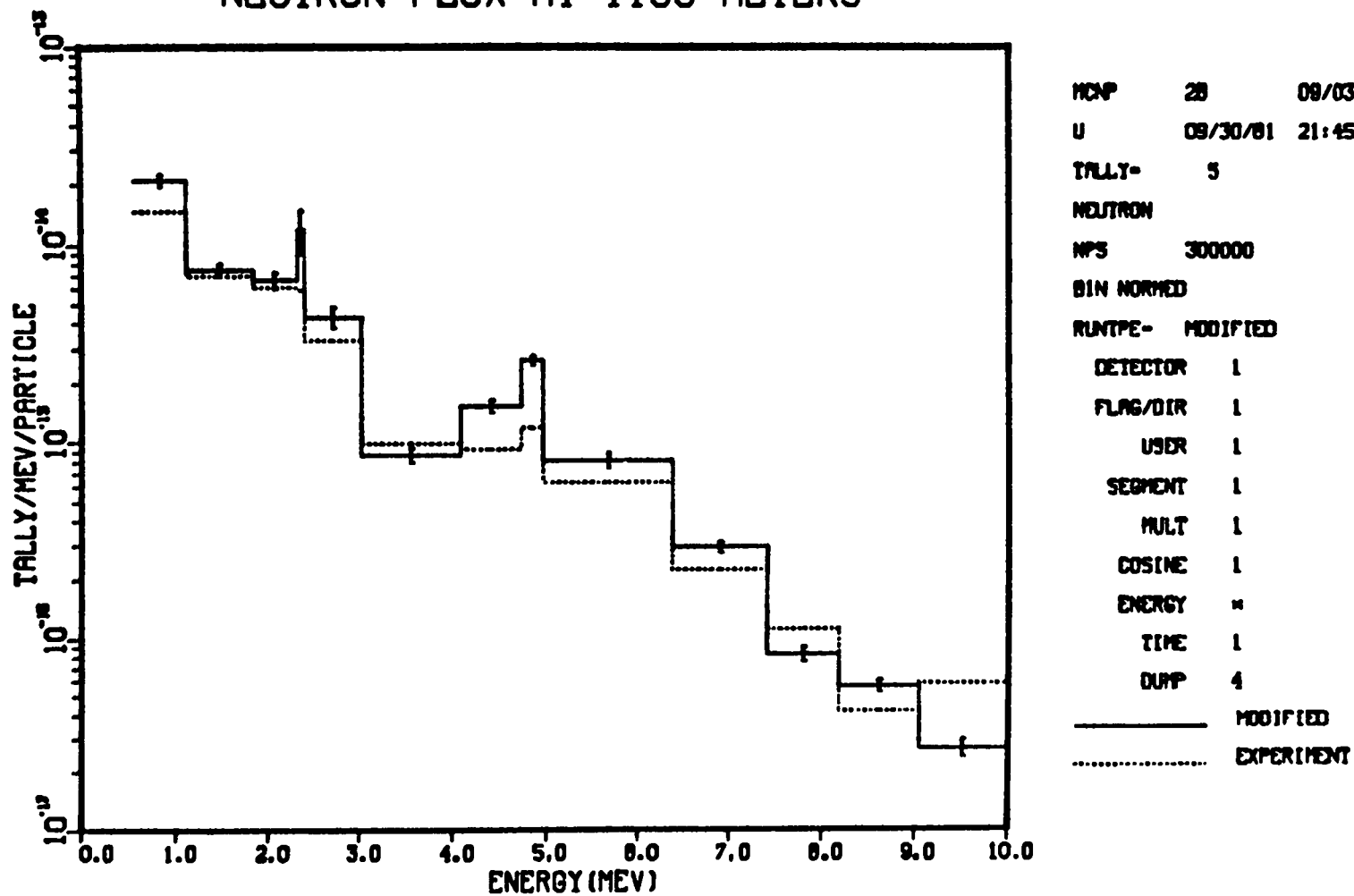
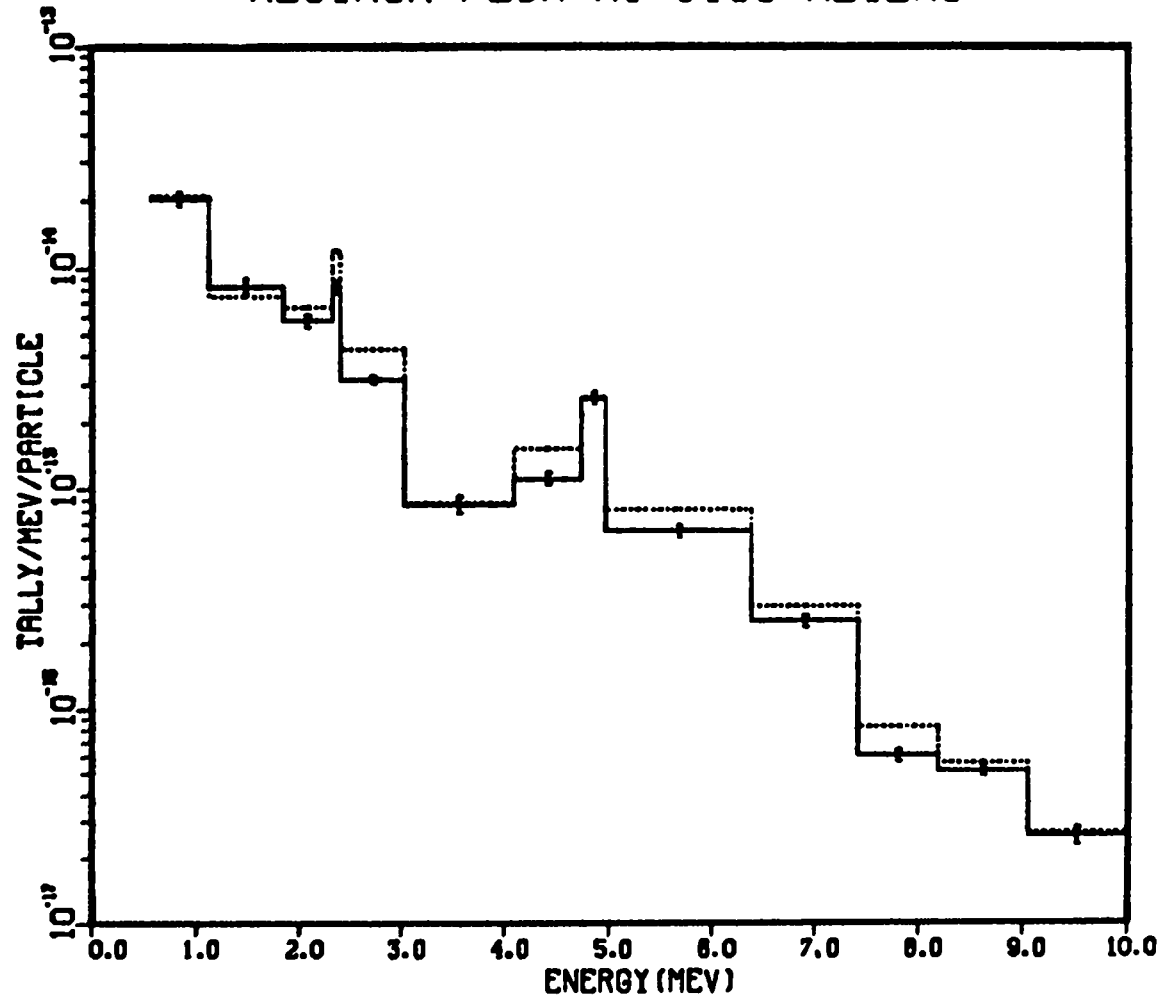


Fig. 31. Neutron flux at 1100 m calculated using modified N-14 and O-16 cross sections compared with DREO experiment.

NEUTRON FLUX AT 1100 METERS



```

MCP      28      09/03/81
T        09/10/81 19:51:53
TALLY=   5
NEUTRON
NPS      300000
BIN NORMED
RUNTPE=  ENDF/B-V
DETECTOR  1
FLAG/DIR  1
USER      1
SEGMENT   1
MULT      1
COSINE    1
ENERGY    4
TIME      1
DUMP      5
-----  ENDF/B-V
.....  MODIFIED
    
```

Fig. 32. Neutron flux at 1100 m calculated using ENDF/B-V and modified N-14 and O-16 cross sections.

NEUTRON FLUX AT 1100 METERS

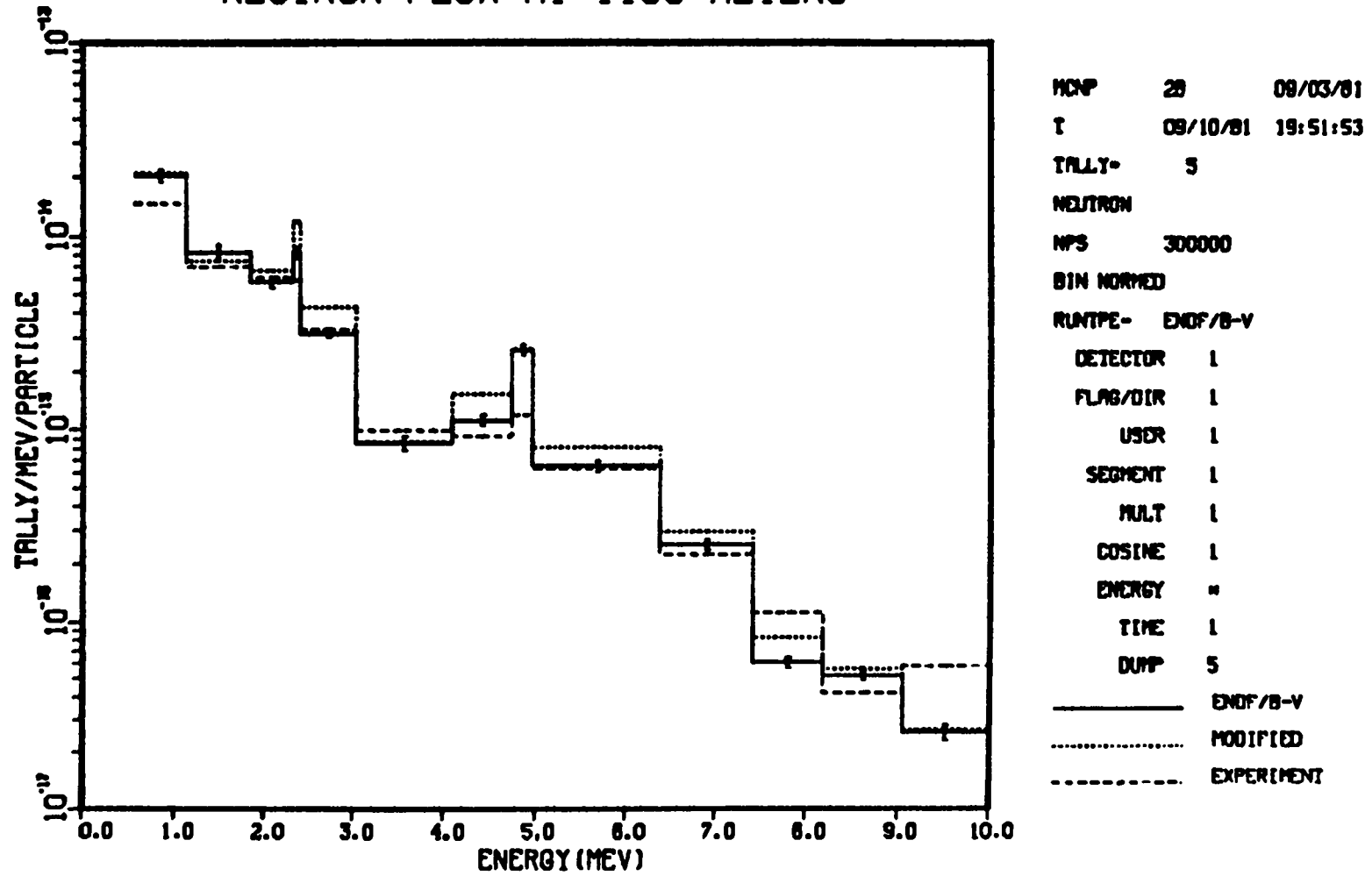


Fig. 33. Neutron flux at 1100 m calculated using ENDF/B-V and modified N-14 and O-16 cross sections compared with DREO experiment.

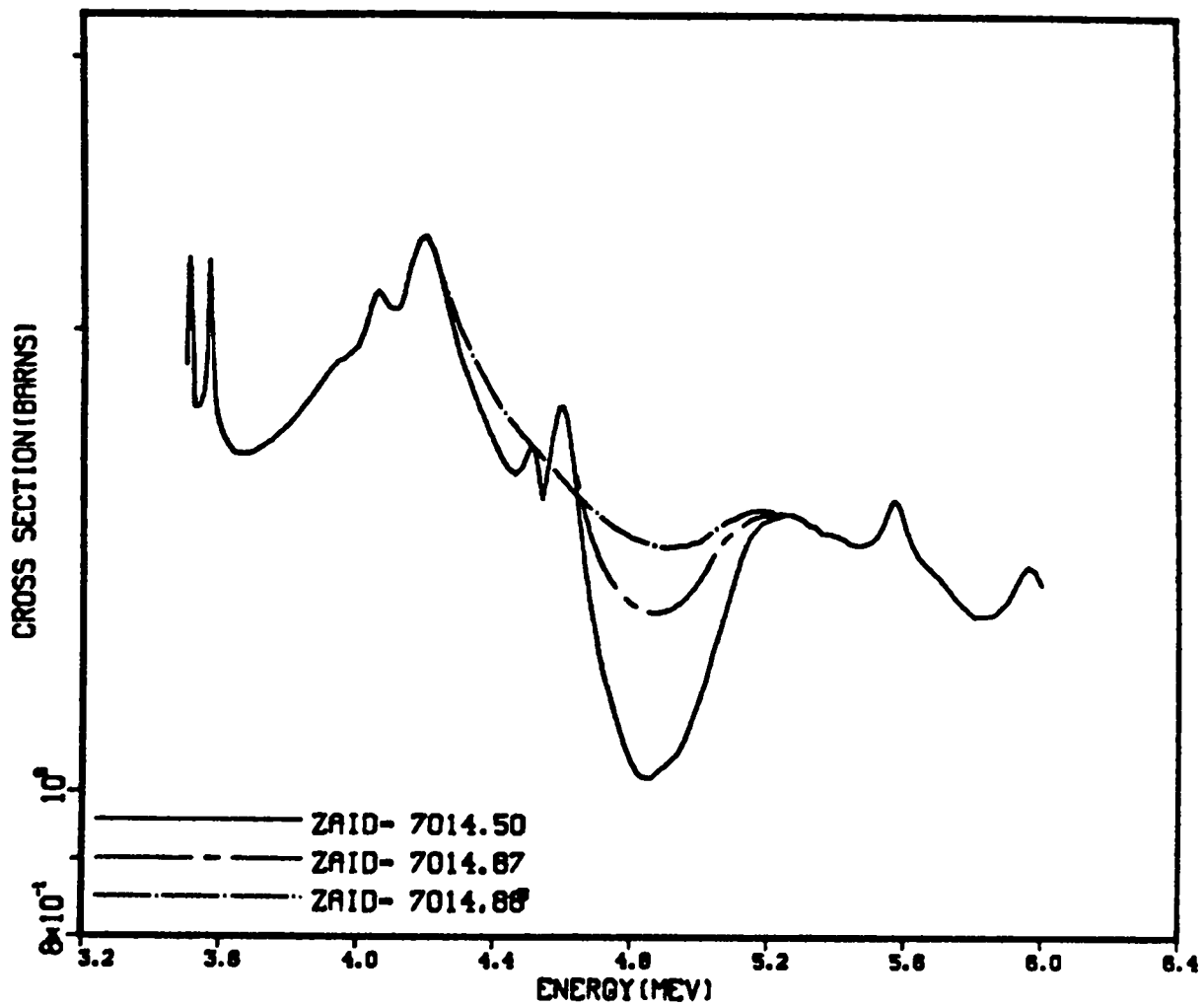


Fig. 34. Two cross-section sets in which the N-14 window at 5 MeV has been removed.

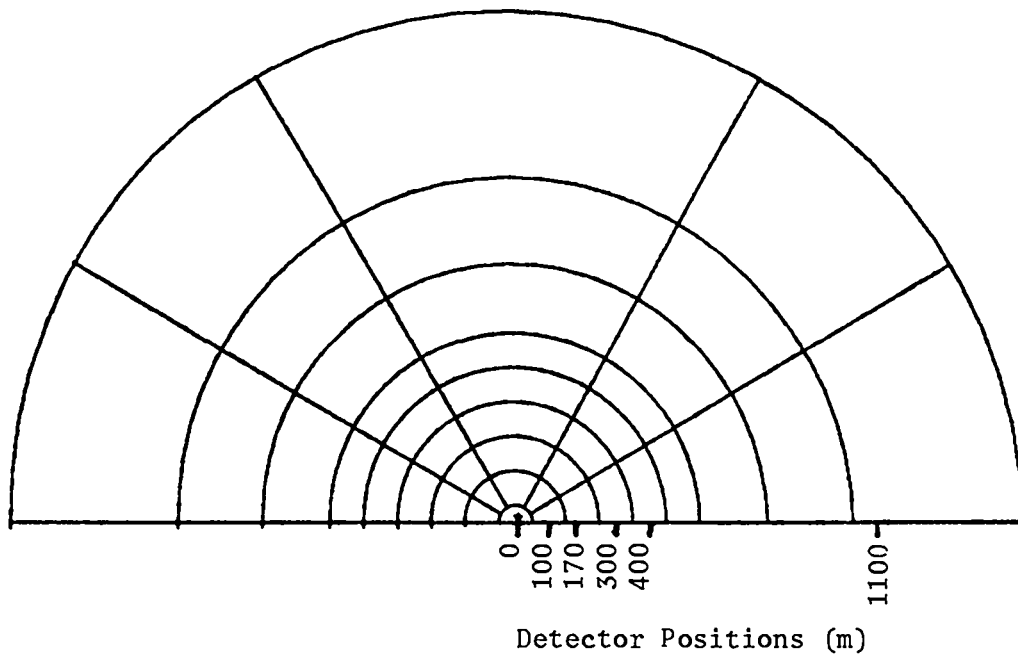


Fig. 35. MCNP geometry model of APRD experiment.

GROUND WATER EFFECTS, 300M

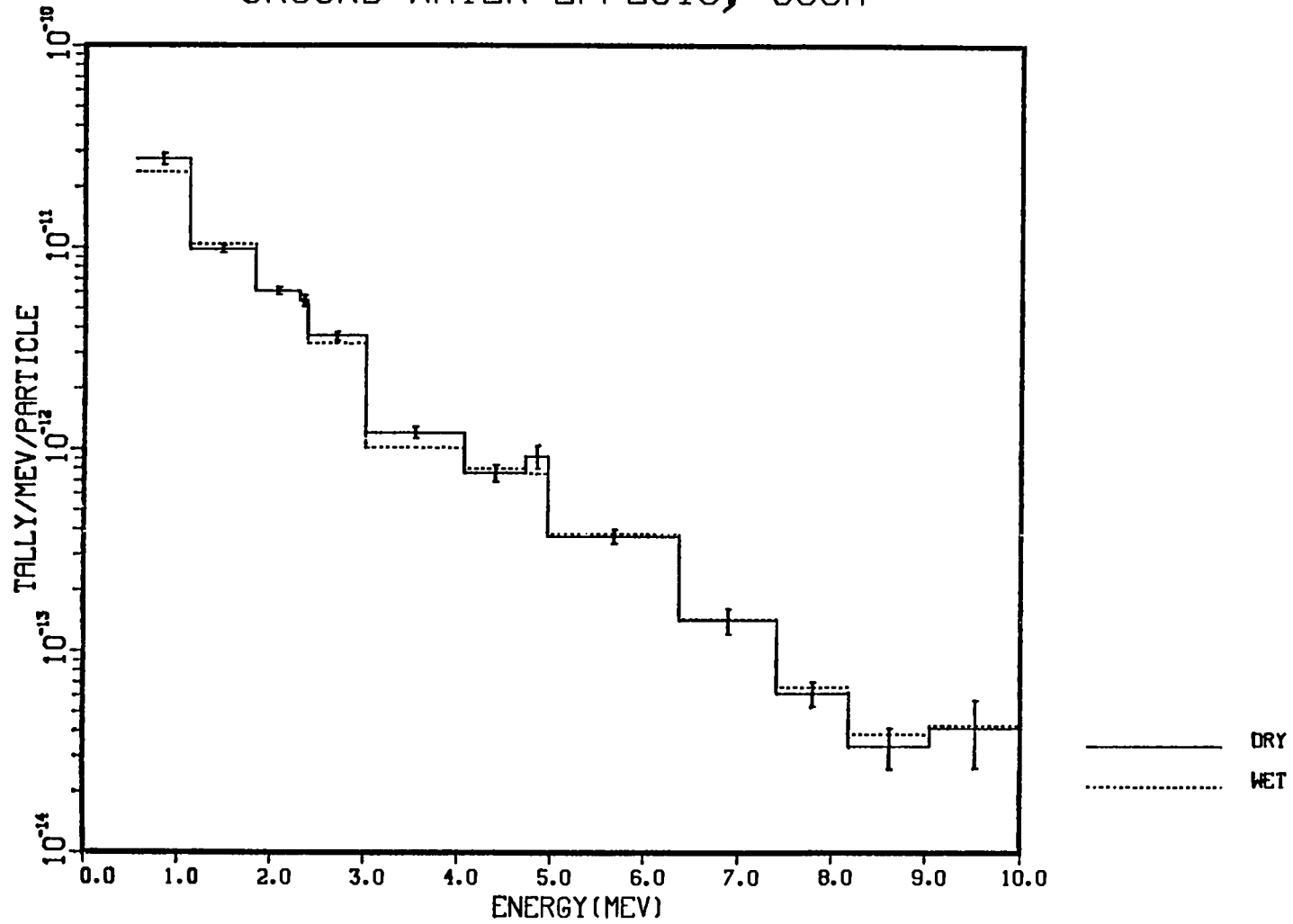


Fig. 36. Effect of dry and wet ground composition on neutron spectrum at 300 m.

GROUND DENSITY EFFECTS, 300M

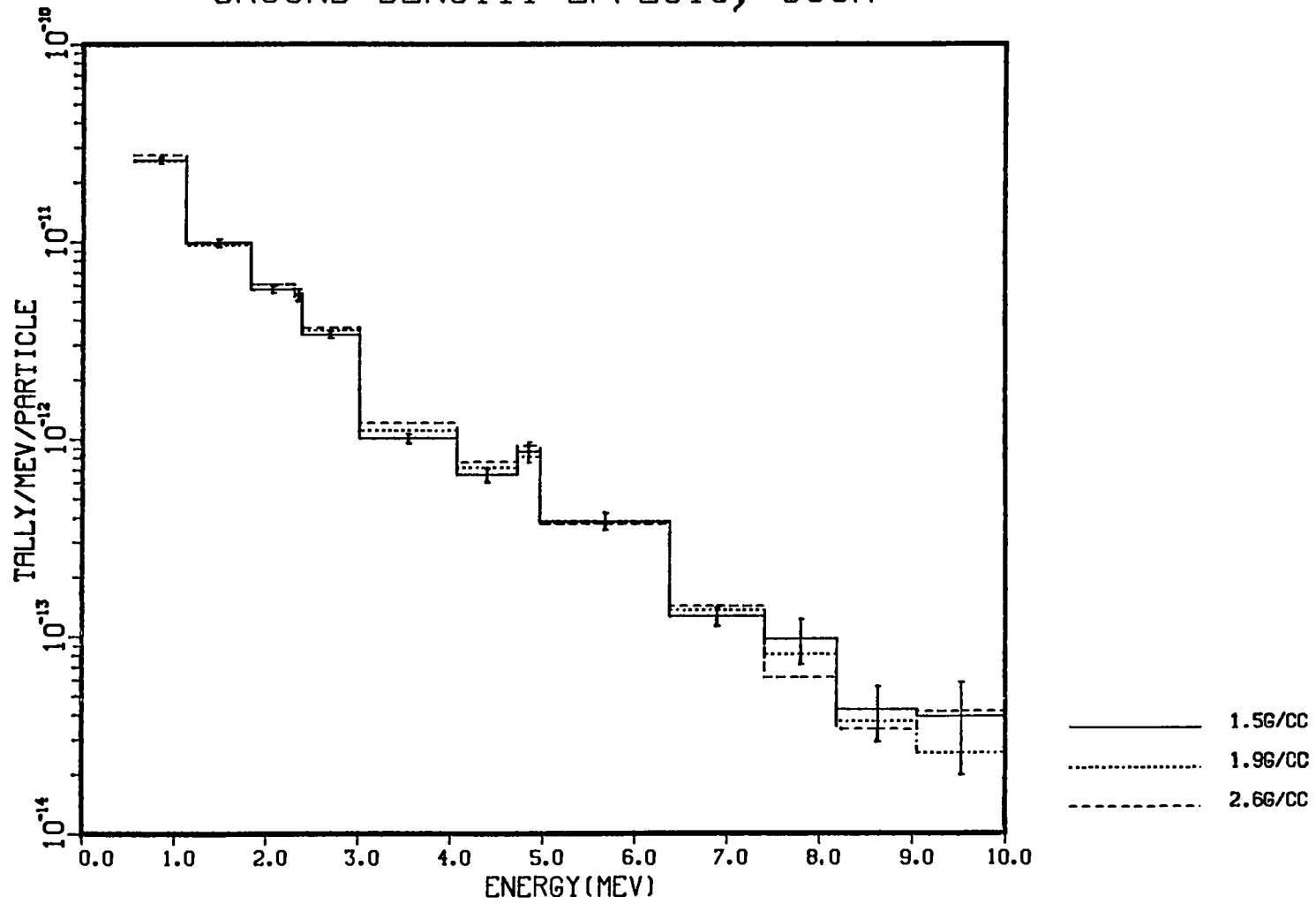


Fig. 37. Effect of ground density changes on neutron spectrum at 300 m.

AIR RELATIVE HUMIDITY EFFECTS, 100M

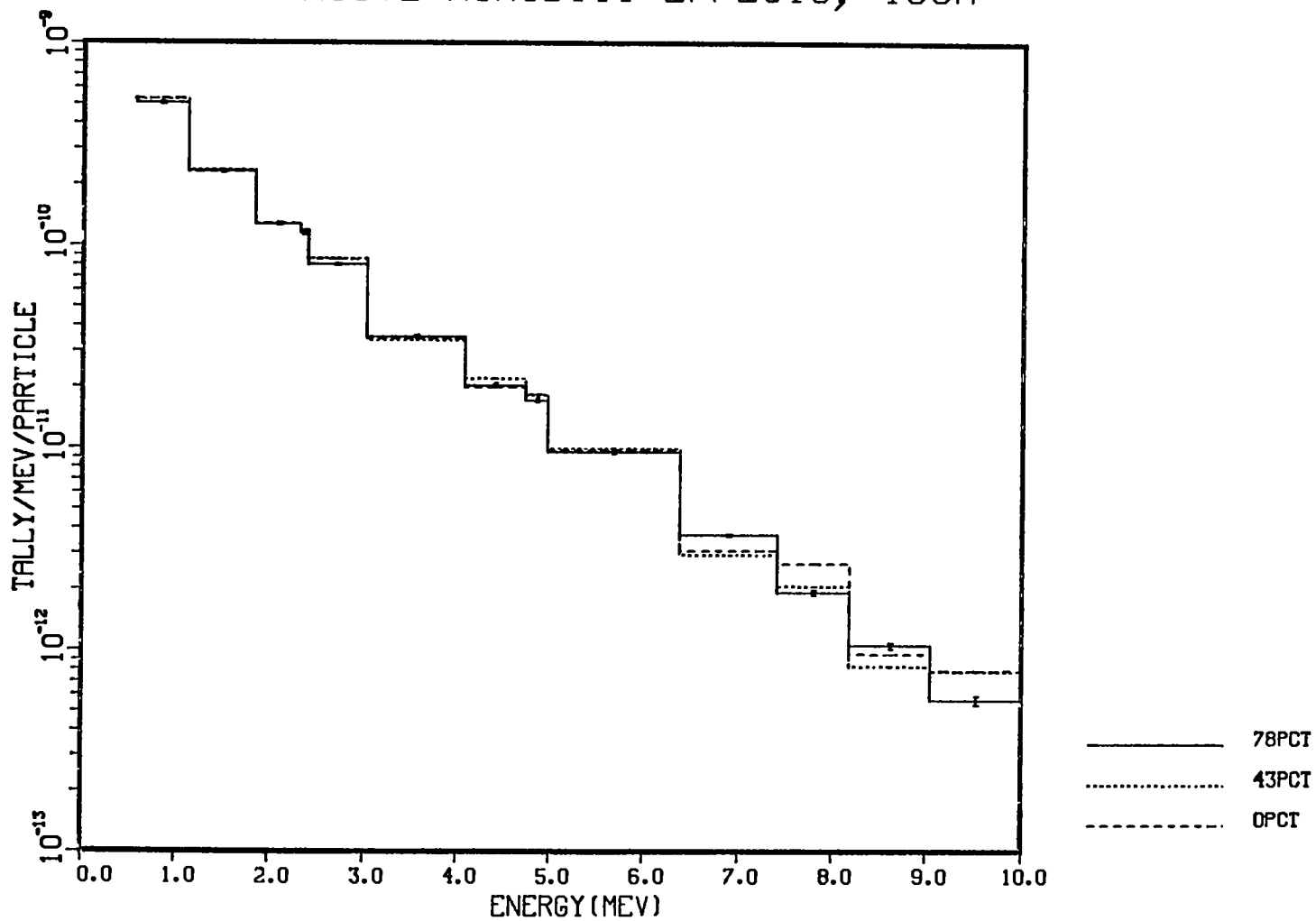


Fig. 38. Effect of relative humidity of air on neutron spectrum at 100 m.

AIR RELATIVE HUMIDITY EFFECTS, 300M

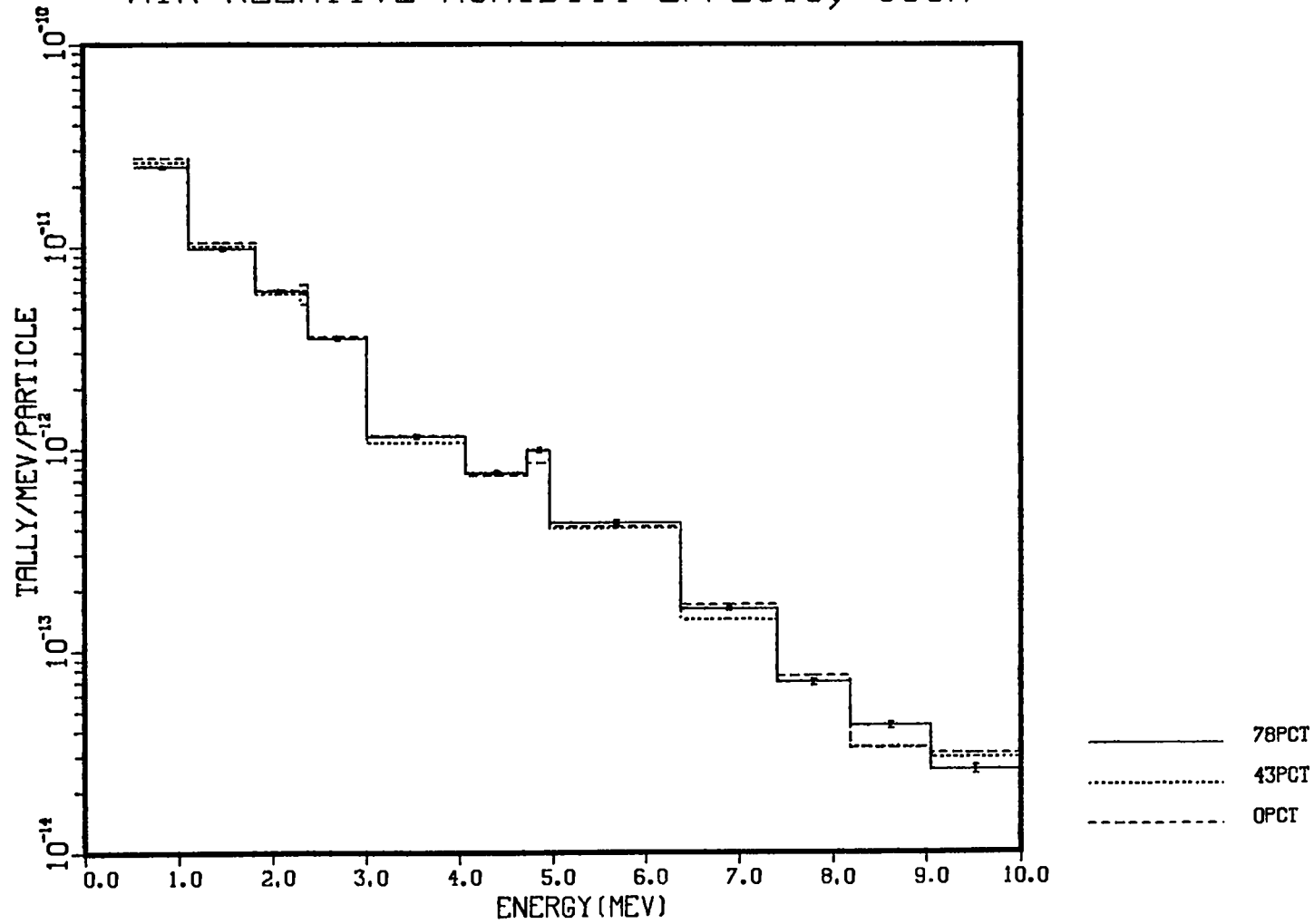


Fig. 39. Effect of relative humidity of air on neutron spectrum at 300 m.

APRD REACTOR NEUTRON SPECTRUM MEASUREMENTS

CALCULATIONS VS. EXPERIMENT AVERAGE

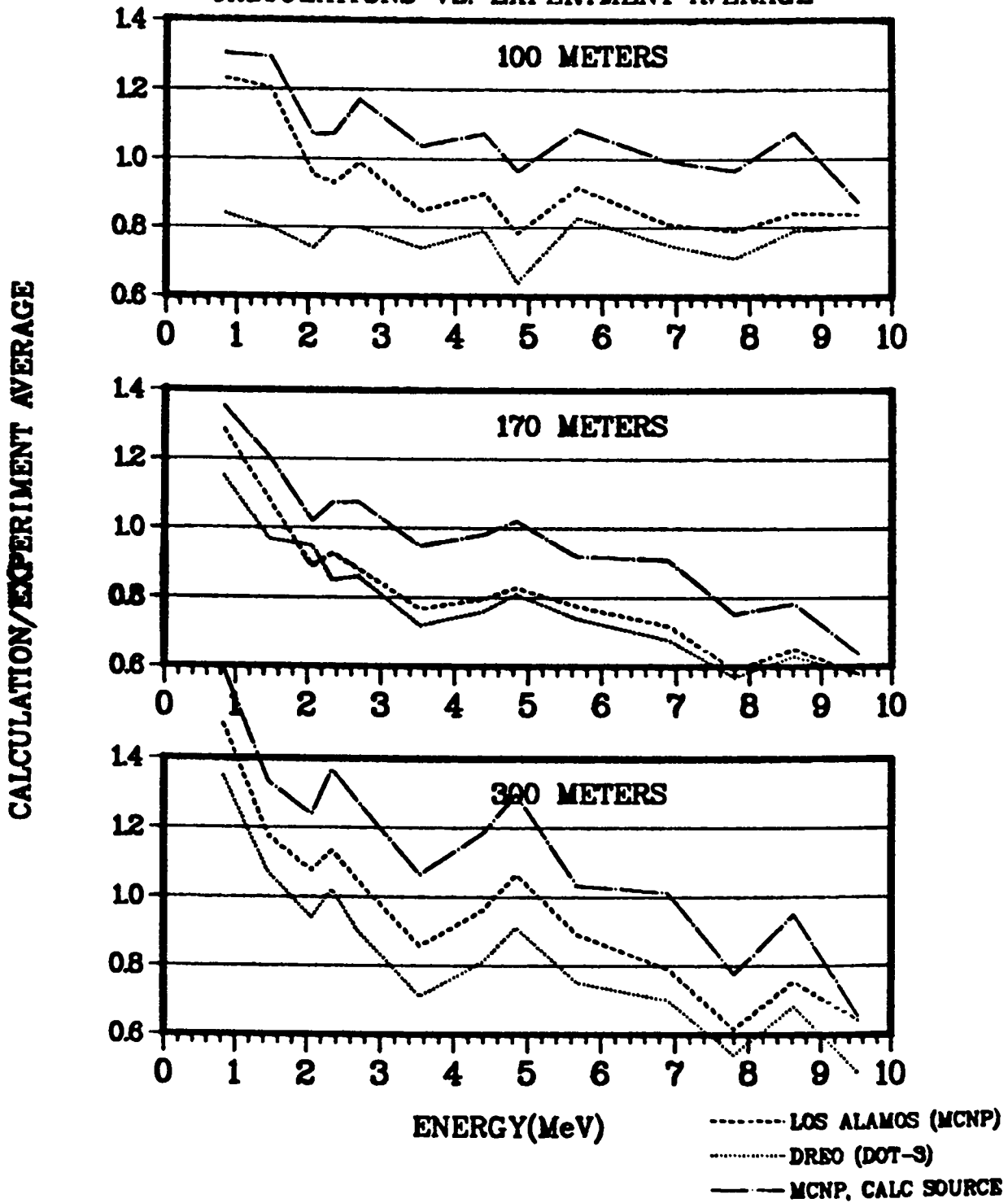


Fig. 40. Neutron spectrum measurements divided by experimental average calculated using modified neutron source spectrum compared with original MCNP and DOT calculations at 100, 170, and 300 m.

APRD REACTOR NEUTRON SPECTRUM MEASUREMENTS CALCULATIONS VS. DREO EXPERIMENT

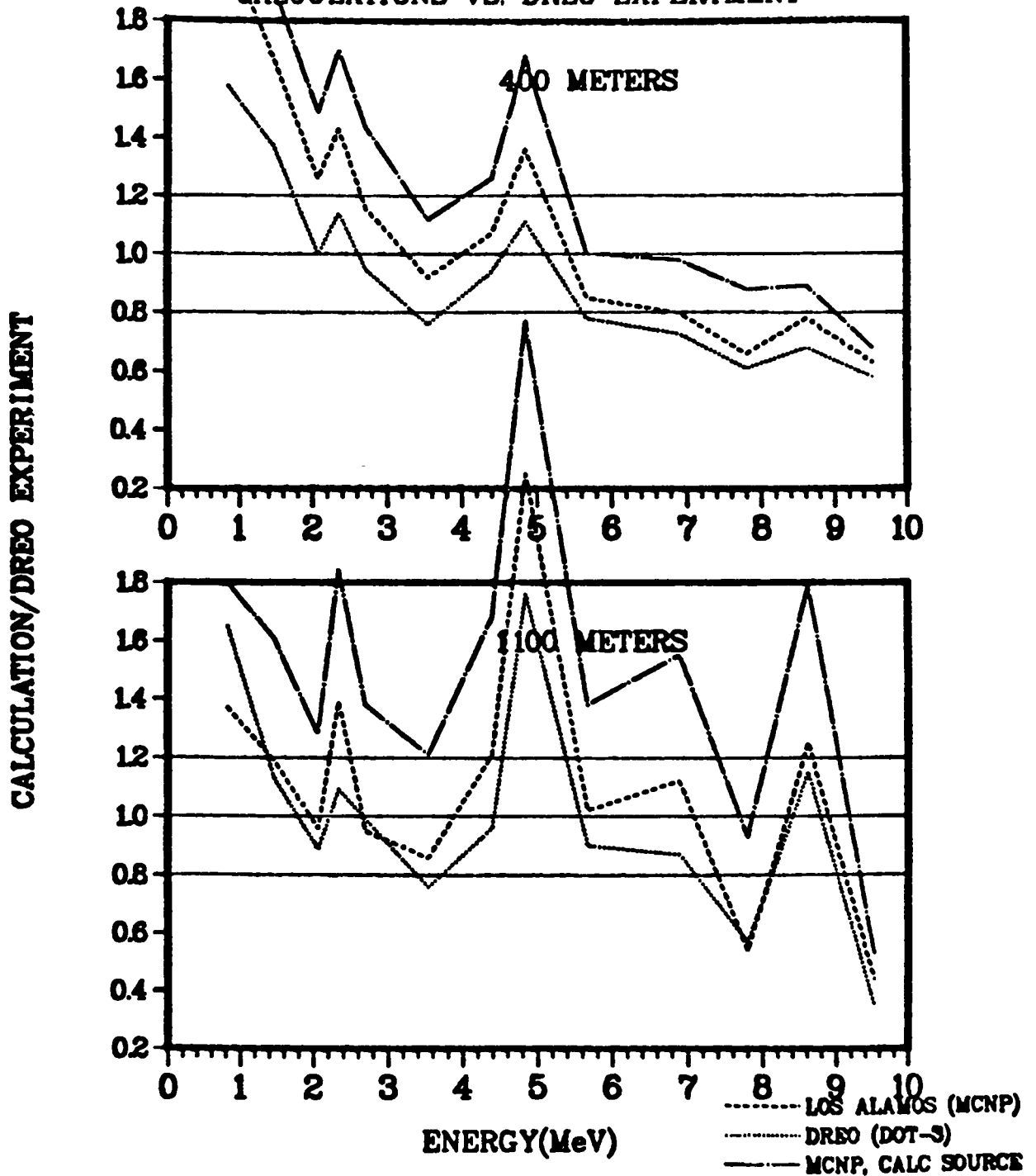


Fig. 41. Neutron spectrum measurements divided by DREO measured results calculated using modified neutron source spectrum compared with original MCNP and DOT calculations at 400 and 1100 m.

TABLE I
 APRD NEUTRON KERMA MEASUREMENTS
 (0.55 MeV - 10 MeV)

| Detector Location (m) | $\frac{\text{DOT Calc.}}{\text{DREO Exp.}}$ | $\frac{\text{MCNP Calc.}}{\text{DREO Exp.}}$ | $\frac{\text{APRD Exp.}}{\text{DREO Exp.}}$ | $\frac{\text{WWD Exp.}}{\text{DREO Exp.}}$ |
|-----------------------------|---|--|---|--|
| 100 | .89 | 1.20 | 1.15 | 1.22 |
| 170 | 1.08 | 1.18 | 1.29 | 1.15 |
| 300 | 1.28 | 1.44 | 1.50 | 1.19 |
| 400 | 1.19 | 1.47 | ---- | ---- |
| 1100 | 1.17 | 1.17 | ---- | ---- |

TABLE II
 ENDF/B-V DATA TESTING RESULTS FOR
 LIVERMORE PULSED SPHERE EXPERIMENTS

| <u>Material</u> | <u>Ref.</u> | <u>Mean Free Path</u> | <u>Angle</u> | <u>LLL Exp. Number</u> | <u>Total (C-E)/E (%)</u> |
|-----------------|-------------|-----------------------|--------------|------------------------|--------------------------|
| Li-6 | 21 | 0.5 | 26 | 102506 | 4.5 |
| | 21 | 1.0 | 26 | 102605 | 4.3 |
| | 22 | 1.0 | | | 4.0 |
| | 21 | 1.6 | 26 | 102606 | 5.3 |
| Li-7 | 21 | 0.5 | 26 | 102507 | 1.8 |
| | 21 | 1.0 | 26 | 102509 | 1.5 |
| | 22 | 1.1 | | | 1.4 |
| | 21 | 1.6 | 26 | 102603 | -0.1 |
| Be-9 | 23 | 1.0 | 26 | 102703 | 7.9 |
| N-14 | 27 | 1.1 | 30 | 17 | -0.6 |
| | 27 | 3.1 | 30 | 18 | 1.5 |
| | 27 | 7.7 | 26 | 41707 | -12.9 |
| O-16 | 27 | 0.7 | 30 | 19 | 5.0 |
| Al-27 | 23 | 0.9 | 30 | 24 | -5.5 |
| | 24 | 0.9 | 30 | 24 | 3.1 |
| Ti | 23 | 1.2 | 30 | 28 | 0.2 |
| | 24 | 1.2 | 30 | 28 | 4.0 |
| Fe | 21 | 0.9 | 30 | 090110 | 2.3 |
| | 22 | 0.9 | | | 2.3 |
| | 21 | 3.0 | 30 | 090103 | -1.9 |
| | 22 | 3.0 | | | -1.9 |
| | 21 | 4.8 | 30 | 090108 | -14.3 |
| | 22 | 4.8 | | | -14.2 |
| Th-232 | 23 | 1.0 | 26 | 102808 | 5.7 |
| | 24 | 1.0 | 26 | 102808 | 5.8 |
| U-235 | 23 | 0.7 | 26 | 102807 | 0.8 |
| | 24 | 0.7 | 26 | 102807 | 0.9 |
| | 23 | 1.5 | 26 | 102810 | 4.0 |
| | 24 | 1.5 | 26 | 102810 | 4.4 |
| U-238 | 23 | 0.8 | 26 | 102806 | 2.6 |
| | 24 | 0.8 | 26 | 102806 | 2.8 |
| | 23 | 2.8 | 26 | 102704 | 1.2 |
| | 24 | 2.8 | 26 | | 1.5 |
| Pu-239 | 23 | 0.7 | 26 | 102804 | -0.4 |
| | 24 | 0.7 | 26 | 102804 | -0.3 |
| CH2 | 21 | 0.8 | 26 | 100311 | -0.1 |
| | 22 | 0.8 | | | -0.1 |
| D20 | 21 | 1.2 | 30 | 42 | -3.0 |
| | 22 | 1.2 | | | -3.0 |
| | 21 | 2.1 | 30 | 43 | 6.2 |
| | 22 | 2.1 | | | 6.2 |
| H20 | 27 | 1.1 | 30 | 39 | -2.3 |
| | 27 | 1.9 | 30 | 40 | 8.8 |

TABLE III

INTEGRAL RESULTS FOR LIVERMORE PULSED SPHERE EXPERIMENTS

| <u>Material</u> | <u>Mean Free Path</u> | <u>Angle</u> | <u>LLL Exp. Number</u> | <u>Fig.</u> | <u>(C-E)/E (%)</u> | | | | |
|-----------------|-----------------------|--------------|------------------------|-------------|--------------------|------------------|------------------|-----------------|----------------|
| | | | | | <u>2-16 MeV</u> | <u>13-16 MeV</u> | <u>10-13 MeV</u> | <u>5-10 MeV</u> | <u>2-5 MeV</u> |
| Oxygen | 0.7 | 30 | 19 | 13 | 5.0 | -1.7 | -14.6 | 36.8 | 53.3 |
| Nitrogen | 1.1 | 30 | 17 | 14 | -0.6 | -7.7 | -17.6 | 32.7 | 42.7 |
| | 3.1 | 30 | 18 | 15 | 1.5 | -10.8 | -25.1 | 19.0 | 33.6 |
| | 7.7 | 26 | 41707 | 16 | -12.9 | -32.3 | -41.7 | -8.5 | 8.2 |
| Water | 1.1 | 30 | 39 | 17 | -2.3 | -8.2 | -4.2 | 11.2 | 13.8 |
| | 1.9 | 30 | 40 | 18 | 8.8 | 3.1 | 5.7 | 15.9 | 19.0 |

TABLE IV

LIQUID AIR PULSED SPHERE CALCULATIONAL RESULTS

LLL Exp. 40104; 7.0 mfp; Detector at 26

| | (C-E)/E (%) | | | | |
|-----------|-------------|-----------|-----------|----------|---------|
| | 2-16 MeV | 13-16 MeV | 10-13 MeV | 5-10 MeV | 2-5 MeV |
| ENDL-73 | -10.5 | -28.5 | -31.5 | -4.6 | 0.9 |
| ENDF/B-IV | -2.5 | -29.7 | -31.7 | 5.9 | 14.2 |

Table V
 MODIFICATIONS IN σ_{tot} FOR N-14 CROSS SECTIONS
 AS FOUND ON FILE N14F

| <u>Energy Interval (MeV)</u> | <u>Number of Energies</u> | <u>Largest Percent Change</u> |
|----------------------------------|-------------------------------|-----------------------------------|
| 0.9 <u><E<</u> 0.988 | 21 | 21.4 % at 0.966 MeV |
| 1.425 <u><E<</u> 1.586 | 19 | 18.3 % at 1.56 MeV |
| 1.610 <u><E<</u> 1.760 | 21 | 13.1 % at 1.66 MeV |
| 1.810 <u><E<</u> 2.10 | 14 | 13.1 % at 1.85 MeV |
| 2.962 <u><E<</u> 3.08 | 17 | 13.4 % at 2.966 MeV |
| 3.095 <u><E<</u> 3.18 | 11 | 6.4 % at 3.15 MeV |
| 3.23 <u><E<</u> 4.28 | 96 | 25.8 % at 3.485 MeV |
| | | 17.5 % at 3.523 MeV |
| | | 16.2 % at 3.595 MeV |
| | | -2.9 % at 4.05 MeV |
| | | -5.1 % at 4.18 MeV |
| 4.304 <u><E<</u> 4.80 | 34 | -5.8 % at 4.52 MeV |
| | | 10.5 % at 4.62 MeV |

TABLE VI
 MODIFICATIONS IN σ_{tot} FOR N-14 CROSS SECTIONS
 AS FOUND ON FILE N14FF

| <u>Energy Interval (MeV)</u> | <u>Uniform Percent Change</u> |
|------------------------------|-------------------------------|
| 0.9 $\leq E \leq$ 1.096 | Increased by 5 % |
| 1.222 $\leq E \leq$ 2.190 | Increased by 7 % |
| 2.964 $\leq E \leq$ 4.820 | |
| 2.964 - 3.50 | Increased by 10 % |
| 3.500 - 3.64 | Increased by 20 % |
| 4.020 - 4.82 | Decreased by 7 % |
| 5.46 $\leq E \leq$ 7.00 | Decreased by 2.5 % |
| 7.50 $\leq E \leq$ 8.40 | Decreased by 2 % |

TABLE VII
 MODIFICATIONS IN σ_{tot} FOR 0-16 CROSS SECTIONS
 AS FOUND ON FILE 016F

| <u>Energy Interval (MeV)</u> | <u>Percent Change</u> |
|------------------------------|--|
| 1.45 \leq E \leq 2.0 | Increased by \approx 10% with maximum change 26% at E = 1.822 MeV |
| 2.24 \leq E \leq 4.74 | Decreased by 20% and 10% |
| 5.34 \leq E \leq 7.50 | Decreased by 6% and 3% |

TABLE VIII

TRANSMITTED FLUX IN NITROGEN BROOMSTICK
CALCULATED USING FIVE AVAILABLE CROSS-SECTION SETS

| E (MeV) | Data ^a | Calculation | | | | |
|---------|-------------------|-------------|---------|------------------------------|---------|---------|
| | | 7014.01 | 7014.02 | Identifying ZAIID 7014.04 | 7014.30 | 7014.50 |
| 0.5000 | | 1.2497 | 1.2497 | 1.2637 | 1.2497 | 1.2634 |
| 0.7507 | ≈5 | 4.7239 | 4.7239 | 4.7708 | 4.7239 | 4.7705 |
| 1.0002 | 6.5 | 8.1230 | 8.1230 | 8.3206 | 8.1230 | 8.3198 |
| 1.2509 | 4.2 | 4.2962 | 4.2962 | 4.4457 | 4.2962 | 4.4457 |
| 1.5005 | 1.9 | 2.2457 | 2.2457 | 2.2851 | 2.2457 | 2.2851 |
| 1.7500 | 2.3 | 2.9649 | 2.9649 | 2.9590 | 2.9649 | 2.9590 |
| 2.0007 | 4.0 | 5.0049 | 5.0049 | 5.0117 | 5.0049 | 5.0117 |
| 2.2503 | 6.0 | 5.9672 | 5.9674 | 6.0043 | 5.9673 | 6.0045 |
| 2.5010 | 6.5 | 6.1231 | 6.1249 | 6.1660 | 6.1231 | 6.1664 |
| 2.7505 | 5.0 | 5.1720 | 5.1788 | 5.1911 | 5.1720 | 5.1914 |
| 3.0001 | 3.0 | 3.2716 | 3.2810 | 3.2899 | 3.2716 | 3.2901 |
| 3.2508 | 1.5 | 1.8785 | 1.8834 | 1.9009 | 1.8785 | 1.9012 |
| 3.5003 | 0.6 | 1.2299 | 1.2308 | 1.2500 | 1.2299 | 1.2503 |
| 3.7499 | .45 | .82254 | .82260 | .84016 | .82253 | .84044 |
| 4.0006 | .65 | .63682 | .63683 | .65113 | .63681 | .65128 |
| 4.2501 | 1.5 | .90427 | .90427 | .92209 | .90426 | .92214 |
| 4.5008 | 2.3 | 1.7597 | 1.7597 | 1.7754 | 1.7597 | 1.7754 |
| 4.7504 | 2.8 | 2.6672 | 2.6672 | 2.6679 | 2.6671 | 2.6680 |
| 5.0011 | 2.7 | 2.7470 | 2.7470 | 2.7321 | 2.7470 | 2.7322 |
| 5.2506 | 1.9 | 2.0949 | 2.0948 | 2.0658 | 2.0948 | 2.0658 |
| 5.5002 | 1.4 | 1.5337 | 1.5337 | 1.4949 | 1.5337 | 1.4949 |
| 5.7509 | 1.3 | 1.3188 | 1.3187 | 1.2883 | 1.3189 | 1.2883 |
| 6.0004 | 1.3 | 1.2508 | 1.2505 | 1.2383 | 1.2519 | 1.2384 |
| 6.2500 | 1.4 | 1.2342 | 1.2340 | 1.2303 | 1.2389 | 1.2303 |
| 6.5007 | 1.4 | 1.2547 | 1.2548 | 1.2504 | 1.2668 | 1.2503 |
| 6.7502 | 1.3 | 1.2216 | 1.2220 | 1.2186 | 1.2423 | 1.2186 |
| 7.0009 | 1.0 | 1.0496 | 1.0501 | 1.0525 | 1.0753 | 1.0525 |
| 7.2505 | 0.8 | .78945 | .78982 | .79737 | .81411 | .79732 |
| 7.5000 | 0.6 | .56945 | .56960 | .57849 | .58927 | .57847 |
| 7.7496 | .48 | .45767 | .45762 | .46570 | .47204 | .46570 |
| 8.0003 | .48 | .43035 | .43005 | .43645 | .44012 | .43645 |
| 8.2498 | .47 | .43025 | .42955 | .43349 | .43657 | .43350 |
| 8.5005 | .43 | .41366 | .41255 | .41473 | .41744 | .41473 |
| 8.7501 | .35 | .37022 | .36898 | .37127 | .37225 | .37127 |
| 8.9996 | .30 | .31295 | .31196 | .31527 | .31398 | .31527 |
| 9.2503 | .25 | .25544 | .25489 | .25879 | .25599 | .25879 |
| 9.4999 | .21 | .20377 | .20354 | .20732 | .20408 | .20732 |
| 9.7506 | .17 | .15905 | .15899 | .16213 | .15921 | .16213 |
| 10.000 | .14 | .12310 | .12308 | .12522 | .12316 | .12522 |

^aApproximate numbers read from Fig. 2 of Ref. 17.
Entries are in neutrons.MeV⁻¹.cm⁻².kW⁻¹.min⁻¹.

TABLE IX
SIMPLY MODIFIED N-14 AND O-16 CROSS SECTIONS

| <u>Material</u> | <u>ZAID</u> | <u>File Name</u> | <u>Factor on σ_{tot}</u> | <u>Energy Range (MeV)</u> |
|-----------------|-------------|------------------|--|---------------------------|
| N-14 | 7014.90 | N14RL1 | 1.2 | 5.0 - 11.0 |
| N-14 | 7014.91 | N14RL2 | 0.8 | 5.0 - 11.0 |
| N-14 | 7014.92 | N14RL3 | 1.05 | 0.5 - 2.5 |
| N-14 | 7014.93 | N14RL4 | 1.20 | 0.5 - 2.5 |
| O-16 | 8016.90 | O16RL1 | 1.05 | 0.5 - 2.5 |
| O-16 | 8016.91 | O16RL2 | 1.20 | 0.5 - 2.5 |

TABLE X
GIVEN AND CALCULATED LEAKAGE SPECTRUM OF APRD REACTOR

| <u>Group</u> | <u>E_{min}(MeV)</u> | <u>E_{max}(MeV)</u> | <u>Leakage Fraction</u> | | <u>Calc/Given</u> |
|--------------|-----------------------------|-----------------------------|-------------------------|-------------------|-------------------|
| | | | <u>Given</u> | <u>Calculated</u> | |
| 1 | 16.9 | 19.64 | | 3.781-7 | |
| 2 | 14.92 | 16.9 | 1.-5 | 1.286-5 | 1.286 |
| 3 | 14.19 | 14.92 | 2.-5 | 2.370-5 | 1.185 |
| 4 | 13.84 | 14.19 | 2.-5 | 7.986-6 | .399 |
| 5 | 12.84 | 13.84 | 6.-5 | 5.849-5(14%) | .975 |
| 6 | 12.21 | 12.84 | 7.-5 | 6.362-5 | .909 |
| 7 | 11.05 | 12.21 | 2.3-4 | 2.354-4 | 1.023 |
| 8 | 10.0 | 11.05 | 4.5-4 | 5.131-4(5%) | 1.140 |
| 9 | 9.048 | 10.0 | 9.8-4 | 1.066-3 | 1.088 |
| 10 | 8.187 | 9.048 | 1.59-3 | 2.001-3 | 1.258 |
| 11 | 7.408 | 8.187 | 2.63-3 | 3.258-3 | 1.239 |
| 12 | 6.376 | 7.408 | 6.19-3 | 7.645-3 | 1.235 |
| 13 | 4.965 | 6.376 | 2.059-2 | 2.450-2(1%) | 1.190 |
| 14 | 4.724 | 4.965 | 5.47-3 | 6.862-3 | 1.254 |
| 15 | 4.066 | 4.724 | 2.068-2 | 2.574-2 | 1.245 |
| 16 | 3.012 | 4.066 | 5.892-2 | 7.296-2 | 1.238 |
| 17 | 2.385 | 3.012 | 6.184-2 | 7.386-2 | 1.194 |
| 18 | 2.307 | 2.385 | 1.058-2 | 1.136-2 | 1.074 |
| 19 | 1.827 | 2.307 | 7.637-2 | 8.338-2 | 1.092 |
| 20 | 1.108 | 1.827 | 1.750-1 | 1.903-1(.3%) | 1.088 |
| 21 | .5502 | 1.108 | 2.376-1 | 2.390-1 | 1.006 |
| 22 | .1576 | .5502 | 2.581-1 | 2.144-1 | .831 |
| 23 | .1111 | .1576 | 2.460-2 | 1.881-2 | .765 |
| 24 | 5.248-2 | .1111 | 2.483-2 | 1.753-2 | .706 |
| 25 | 2.479-2 | 5.248-2 | 8.91-3 | 4.896-3(2%) | .549 |
| 26 | 2.188-2 | 2.479-2 | 6.7-4 | 3.066-4 | .458 |
| 27 | 1.033-2 | 2.188-2 | 2.54-3 | 8.517-4 | .335 |
| 28 | 3.355-3 | 1.033-2 | 8.9-4 | 2.303-4(10%) | .259 |
| 29 | 1.234-3 | 3.355-3 | 1.6-4 | 1.504-5 | .094 |
| 30 | 5.829-4 | 1.234-3 | 3.-5 | 7.318-7 | .024 |
| 31 | 1.013-4 | 5.829-4 | 1.-5 | 1.203-6 | .120 |

Ratio of Calculated to Given Leakage

| | |
|-----------------------|------|
| Above 3.012 MeV | 1.23 |
| .5502 MeV - 3.012 MeV | 1.07 |
| Below .5502 MeV | .80 |

Printed in the United States of America
Available from
National Technical Information Service
US Department of Commerce
5285 Port Royal Road
Springfield, VA 22161

Microfiche (A01)

| Page Range | NTIS Price Code |
|------------|--------------------|------------|--------------------|------------|--------------------|------------|--------------------|
| 001-025 | A02 | 151-175 | A08 | 301-325 | A14 | 451-475 | A20 |
| 026-050 | A03 | 176-200 | A09 | 326-350 | A15 | 476-500 | A21 |
| 051-075 | A04 | 201-225 | A10 | 351-375 | A16 | 501-525 | A22 |
| 076-100 | A05 | 226-250 | A11 | 376-400 | A17 | 526-550 | A23 |
| 101-125 | A06 | 251-275 | A12 | 401-425 | A18 | 551-575 | A24 |
| 126-150 | A07 | 276-300 | A13 | 426-450 | A19 | 576-600 | A25 |
| | | | | | | 601-up* | A99 |

*Contact NTIS for a price quote.



Los Alamos